LBL-26448

Lawrence Berkeley Laboratory
UNIVERSITY OF CALIFORNIA

Physics Division

Presented at the 1988 Snowmass Summer Study on High Energy Physics in the 1990s, Snowmass, CO, June 24– July 17, 1988, and to be published in the Proceedings

New Particle Signals at the SSC and at an Upgraded Tevatron Collider

R. Michael Barnett, Robert J. Hollebeek, Andrew P. White, John Yoh, Howard A. Baer, Bruce A. Barnett, Estia Eichten, James E. Freeman, Georgio Gamberini, J.A. Grifols, John F. Gunion, Howard E. Haber, John Haggerty, Clemens A. Heusch, JoAnne L. Hewett, Ian Hinchliffe, T. Kamon, S. Kim, A. Méndez, Jean-Pierre Mendiburu, Sergio F. Novaes, Frank E. Paige, Rajendran Raja, Thomas G. Rizzo, Xerxes Tata, and Jeffrey Woodside

January 1989

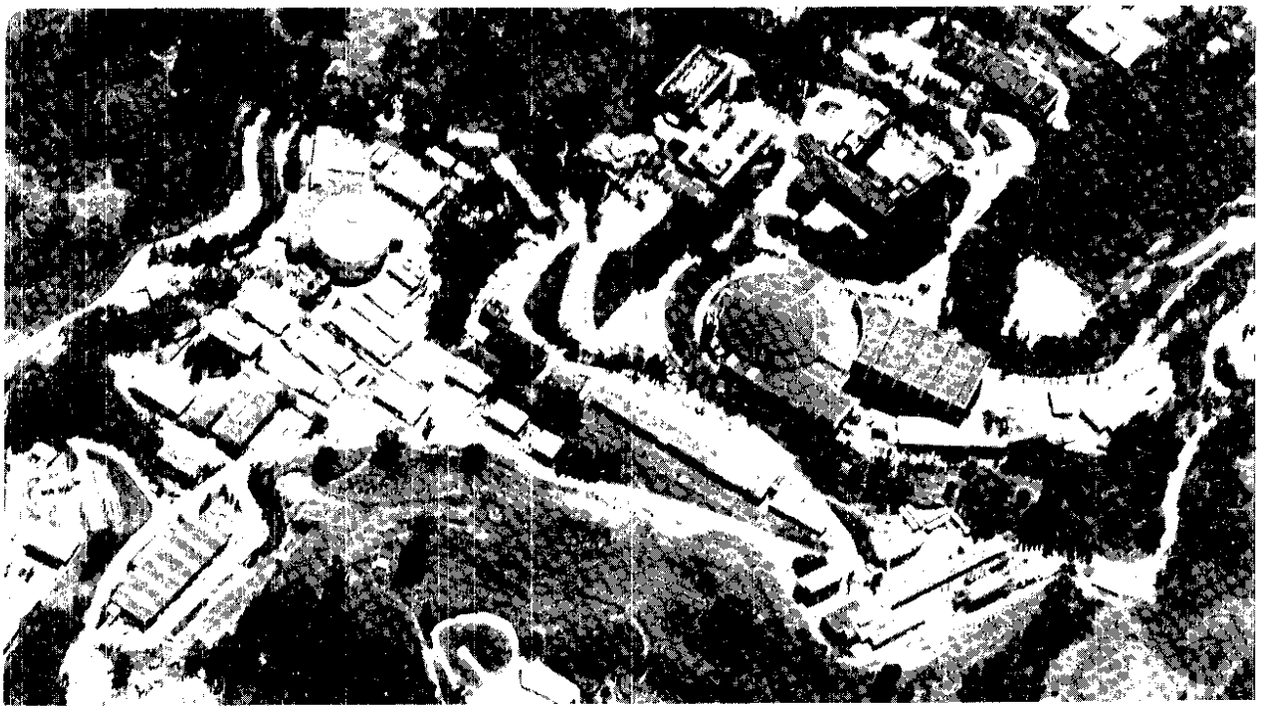

Prepared for the U.S. Department of Energy under Contract Number DE-AC03-76SF00098.

New Particle Signals at the SSC and at an Upgraded Tevatron Collider*

R. MICHAEL BARNETT[a], ROBERT J. HOLLEBEEK[b], ANDREW P. WHITE[c], JOHN YOH[d], HOWARD A. BAER[e], BRUCE A. BARNETT[f], ESTIA EICHTEN[d], JAMES E. FREEMAN[d], GEORGIO GAMBERINI[a], J.A. GRIFOLS[g], JOHN F. GUNION[h], HOWARD E. HABER[i], JOHN HAGGERTY[j], CLEMENS A. HEUSCH[i], JOANNE L. HEWETT[k], IAN HINCHLIFFE[a], T. KAMON[l], S. KIM[l], A. MÉNDEZ[g], JEAN-PIERRE MENDIBURU[m], SERGIO F. NOVAES[a], FRANK E. PAIGE[j], RAJENDRAN RAJA[d], THOMAS G. RIZZO[n], XERXES TATA[o,k], JEFFREY WOODSIDE[p]

[a] *Physics Division, Lawrence Berkeley Laboratory, Berkeley, CA 94720*
[b] *Department of Physics, University of Pennsylvania, Philadelphia, PA 19104*
[c] *Department of Physics, University of Florida, Gainesville, FL 32611*
[d] *Fermilab, Batavia, IL 60510*
[e] *Department of Physics, Florida State University, Tallahassee, FL 32306*
[f] *Department of Physics, Johns Hopkins University, Baltimore, MD 21218*
[g] *Grup de Física Teòrica, UAB, 08193 Bellaterra (Barcelona), Spain*
[h] *Department of Physics, University of California, Davis CA 95616*
[i] *SCIPP, University of California, Santa Cruz, CA 95064*
[j] *Physics Department, Brookhaven National Laboratory, Upton, NY 11973*
[k] *Department of Physics, University of Wisconsin, Madison, WI 53706*
[l] *Inst. of Physics, University of Tsukuba, Ibaraki-ken 305, Japan*
[m] *College de France, Paris, France*
[n] *Ames Lab. and Department of Physics, Iowa State University, Ames, IA 50011*
[o] *Department of Physics and Astronomy, University of Hawaii, HI 96822*
[p] *Department of Physics, Oklahoma State University, OK 74078*

ABSTRACT

We have studied the production and detection of several types of new particles at the Superconducting Super Collider (SSC) and at three possible upgrades of the Fermilab Tevatron Collider. We compare the physics potential of the SSC with that of an upgraded collider, and we discuss in depth the relative capabilities of the three Tevatron Collider upgrades. From a physics standpoint, we suggest that one of the proposed upgrades has several advantages.

* This work was supported by the Director, Office of Energy Research, Office of High Energy and Nuclear Physics, Division of High Energy Physics, of the U.S. Department of Energy under Contract Nos. DE-AC03-76SF00098, DE-AC02-76-ER0-3071, DE-AS03-76ER70191, DE-AA03-76-SF00010, DE-AC02-76ER00881 and W-7405-Eng-82, by the National Science Foundation under agreement no. PHY83-18358, and by the University of Wisconsin Research Committee with funds granted by the Wisconsin Alumni Research Foundation.

1. Introduction

The "New Particles at Hadron Colliders" group had several general tasks.

a) Refine the techniques for finding new particles at the SSC and at an upgraded Tevatron Collider. For the most part we concentrated on those areas where previous studies were inadequate or non-existent.

b) Investigate whether there is a gap between the capabilities of the SSC and the Tevatron. If there is a gap, would an upgraded Tevatron Collider be able to make a significant difference ? It has also been suggested that any gap could be filled by running the SSC at lower energies. The SSC Conceptual Design Report states that the SSC can be run at lower energies with high luminosity (at $\sqrt{s} = 10$ TeV, luminosity would be $5 \times 10^{32}\ cm^{-2}s^{-1}$; at $\sqrt{s} = 3$ TeV, luminosity would be 10^{32}). However, we did not take this possibility into account.

c) Compare three proposed upgrades for the Tevatron Collider. We examined the upgrades to see which allowed the best search limits for various types of new particles and which upgrades could best study any particles which were discovered. It is important to decide which signals are feasible because the branching ratios for each signal is different and can lead to differing conclusions for each upgrade.

The table shows the parameters which were our starting assumptions. Since these are hypothetical upgrades, the parameters may change in time. By "future runs" we refer to Tevatron Collider runs before the upgrades A, B or C.

The new particles discussed here include new heavy leptons for which we show for the first time that they could be observable at the SSC. For new W' and Z' bosons we have concentrated on the possibilities at an upgraded Tevatron Collider. We made an intensive study of supersymmetric particles because of serious deficiencies in previous studies; this work is not complete but the preliminary indication is that techniques for finding gluinos and squarks do exist. We looked carefully at the requirements for finding supersymmetric particles at Tevatron upgrades. Work on new heavy quarks (beyond the top quark) is continuing and is not reported here. Higgs bosons and technicolor were assigned to the Electroweak Symmetry Breaking group at Snowmass and are therefore not included. No new work was done on compositeness (substructure) and on the particles predicted by superstring theories except as they fall into the above categories.

2. Heavy Leptons

2.1. Heavy Lepton Introduction

Heavy leptons are some of the most difficult new particles to find at a hadron collider. Their production rate is small since they must be produced by electro-weak interactions. Backgrounds are very large, and strong cuts are needed to bring them below the signals. Previous studies of the detection prospects have concentrated on the rate and have not studied the backgrounds[1,2] in detail or have concluded that signals cannot be extracted due to the large backgrounds.[3] As described below, Ian Hinchliffe has devised a set of cuts which do, in principle, allow a signal to be established.

Let us consider a fourth generation lepton doublet $\binom{L}{N}$, with L (N) being the charged (neutral) member. We shall further assume that L is heavier than N. Some constraints on the existence of such a doublet exist already. Measurements of the value of W and Z masses and the weak mixing angle imply that $|m_L - m_N| < 310$ GeV (90% confidence).[4] This bound could be upset by other particles added to the standard model. There is a limit $M_L > 41$ GeV (95% confidence) from the UA1 collaboration[5] working at the $Sp\bar{p}S$ collider. This limit arises from the non-observation of electrons from the process $W \to LN \to e\nu N\bar{N}$ and assumes that N is stable and is light.

OPTION		$\sqrt{s}$	$\mathcal{L}$	sec/year	$\int \mathcal{L}\, dt$
A	$p\bar{p}$	2 TeV	2×10^{31}	0.5×10^7	100 pb^{-1}
B	pp	2 TeV	10^{32}	10^7	1000 pb^{-1}
C	$p\bar{p}$	3 TeV	6×10^{30}	0.5×10^7	30 pb^{-1}
This run	$p\bar{p}$	1.8 TeV			$3 - 5$ pb^{-1}
Future runs	$p\bar{p}$	1.8 TeV			$15 - 20$ pb^{-1}?
SSC	pp	40 TeV	10^{33}	10^7	10,000 pb^{-1}

If the N is sufficiently light, it will contribute to the Z width

$$\Gamma(Z \to N\overline{N}) = 160\sqrt{1-4m_L^2/m_Z^2}(1-m_L^2/m_Z^2) \quad MeV.$$

Therefore experiments which count the number of neutrinos will be sensitive to it provided that it is stable. Currently one cannot exclude such a neutrino.[6] However, experiments at LEP should be able either to detect such a lepton or to set a limit of order 40 GeV on its mass.[7] (A better limit can probably be obtained at LEP2, up to 80 GeV or so, but only if the N is unstable). Charged leptons of masses up to 80 GeV or so will be found at LEP2.[7] In the context of a discussion of searches at hadron colliders only the SSC and LHC are relevant. It should be possible to improve the UA1 limit somewhat at the Tevatron collider, but the limiting factor is rate; only leptons accessible in W decay are produced copiously enough to be found.

2.2. Heavy Lepton Discussion and Results

Apart from W decay, which is not relevant to heavy lepton production in high energy colliders, there are four relevant production mechanisms. First, L^+L^- or LN pairs can be made by quark antiquark annihilation via a virtual Z/γ or W. The rate for this is well predicted, given the L and N masses, since it depends only on the quark and antiquark distribution functions which are well known.[1]

Second, an L^+L^- (or $N\overline{N}$) pair can be produced in a gluon gluon collision via the process shown in Fig. 1.[8]

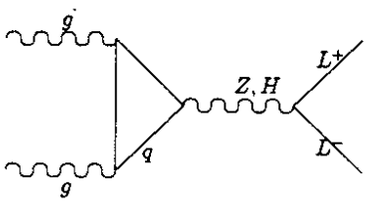

Figure 1. Feynman diagram showing the process $gg \to L^+L^-$. The loop contains a sum over all quark flavors.

The loop contains quarks. The contribution from the virtual Z is zero unless there is a quark doublet the masses of whose members straddle the mass of the virtual Z. The contribution from the Higgs depends on the quark masses, but there are no cancellations between the individual quark contributions. The presence of an additional lepton doublet in the standard model requires the existence of another quark doublet to cancel anomalies. The

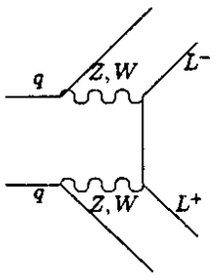

Figure 2. Feynman diagram showing the process $qq \to L^+L^-qq$.

masses of these quarks are very important in determining the production rate from this process.

Third, there is the process $qq \to qqL^+L^-$ via intermediate W's or Z's, see Fig. 2. This process produces a rate which is negligible[9] with respect to the ones from the processes above and is not discussed further.

Fourth, there is the possibility that some other new particle, produced copiously, could decay into the heavy lepton. (Recall the UA1 limit discussed above.) The rate from such a process is very model dependent.

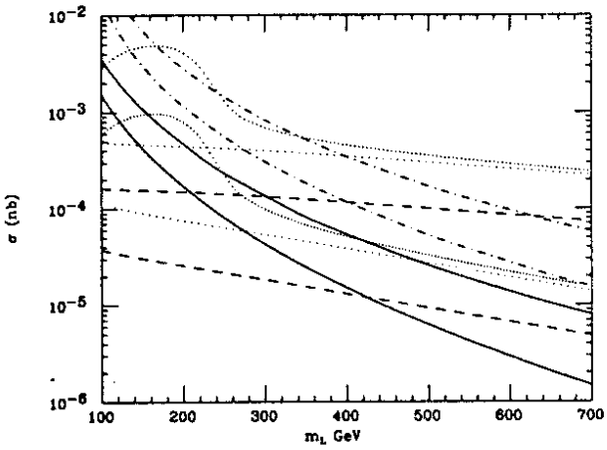

Figure 3. Total cross-sections for heavy lepton production in pp collisions as a function of the charged lepton (L) mass; N is assumed to be massless. A pair of lines is shown for each process; the upper (lower) is for $\sqrt{s} = 40(17)$ GeV. The solid lines are for the process $q\overline{q} \to L^+L^-$ and the dot-dashed for $q\overline{q} \to L^\pm N$ (charges summed). The rates from the process $gg \to L^+L^-$ are shown with $m_H = 100$ GeV and no 4^{th} generation of quarks (dashed lines), $m_H = 100$ GeV and the 4^{th} generation quark masses set to m_L and $m_L + 100$ GeV (dotted lines), and $m_H = 500$ GeV and the 4^{th} generation quark masses set to m_L and $m_L + 100$ GeV (close dotted lines).

Figure 3 shows the total cross-section from the first three of these processes; the formulae are given at the end of this section for completeness. In the case of the third process several lines are shown corresponding to different choices of the Higgs and fourth generation quark

masses. It can be seen from this figure that the rates are of order 1 pb over the interesting range of masses. Notice that the rate from the gluon-gluon process falls relatively slowly with increasing lepton mass. This occurs because the Higgs-lepton coupling is proportional to the lepton mass. The rate is approximately independent of the Higgs mass (m_H) if $m_L > m_H$. If $m_H > m_L$ the rate increases as m_H increases.[8] This can also be seen clearly from Fig. 3 where rates from Higgs masses of 100 and 500 GeV are shown.

It can be seen from this figure that the rate from the gluon-gluon initial state is dominant over most of the relevant range of masses if we are interested in the L^+L^- final state. In what follows we shall take the fourth generation down and up quark masses to be $m(Q_4) = m_L$ and $m_L + 100$ GeV and shall assume $m_H = 100$ GeV. While the rates so obtained are model dependent, they could be larger if either m_H or the splitting between the charge 2/3 and charge 1/3 quarks is larger. The charged lepton L will decay into "W"+N, where the W is real if $m_L - m_N > m_W$ and virtual otherwise. Initially we will assume that N is stable.

Let us consider first the LN final state (which has a larger cross-section than that of the L^+L^- final state if $m_L >> m_N$). This then gives rise to a W and missing transverse momentum, carried off by the N's. If one attempts to detect the W via its *leptonic* decay mode, the signal is now an isolated lepton and missing transverse momentum. This signal is overwhelmed by isolated leptons from the process $q\bar{q} \to l\nu$ via an intermediate W boson.[3] An attempt to detect W decaying *hadronically* faces a background from the final state ZW where the Z decays to neutrinos and the W hadronically. This background is not overwhelming but there is an additional, much more problematic, final state of $Z + jets$ where the Z decays to neutrinos and the jet system is indistinguishable from that arising from a W decay.

Much work[10] has been done on the problem of resolving a W decaying hadronically from a jet system, mostly in the context of searches for the Higgs boson decaying to W^+W^- where one W decays leptonically and the other hadronically. Here the dominant background is $W + jets$. One requires that the invariant mass of the jet system be close to the W. Other methods such as an attempt to resolve the jet system into two jets (due to q and $\bar{q}$ in the W decay case), followed by cuts on the angular distribution of these jets[10], or a cut on the particle multiplicity[11] of the jet system may increase the background rejection somewhat.[12] The multipicity cut is considered because the W decays to quarks whereas the background jet system is mainly gluons; gluon jets are expected to produce larger multiplicity. In the LN case, a cut on the invariant mass of the jet system $m_{jets} = m_W \pm 10$ GeV produces a signal to background ratio of less than 0.1 at $\sqrt{s} = 40$ TeV

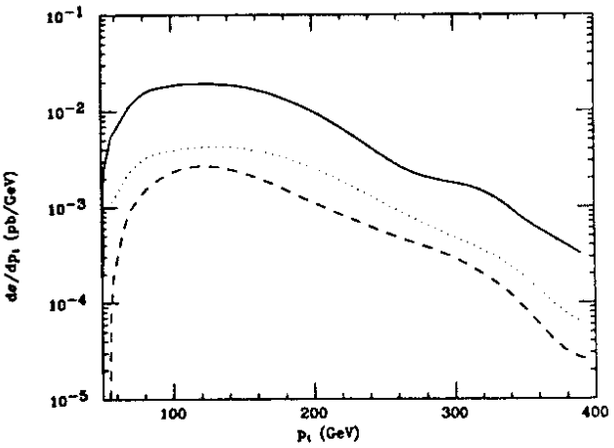

Figure 4. The transverse momentum distribution $d\sigma/dp_t$ for a W boson from the process $pp \to L^{\pm}N + N \to W^{\pm}N\overline{N} + X$ at $\sqrt{s} = 40$ TeV. There is missing transverse momentum which balances that of the W. The W is decayed to $q\bar{q}$ and the following cuts on the rapidity (y), transverse momentum (p_t) and azimuthal angle (ϕ) of the quark and anti-quark made: $|y| < 5$, $p_t > 50$ GeV, $\Delta R\sqrt{((\Delta\phi)^2 + (\Delta y)^2)} > 0.5$. The last cut is an attempt to ensure that the two jets from the quark and antiquark are distinct (ΔR is the separation of the partons). The dotted (dashed) line corresponds to $m_L = 100$ (200) GeV; $m_N = 0$. The solid line is the rate $d\sigma/dp_t$ from the process $pp \to Z(\to \nu\overline{\nu}) + 2partons + X$ shown as a function of p_t of the Z. The two parton system is subject to the same cuts as above. In addition the invariant mass of the system must be in the range $M_W \pm 10$ GeV.

energies. This is shown in Fig. 4 where the background is calculated from the final state Z+2 *partons*. The signal to background ratio is slightly worse at $\sqrt{s} = 17$ TeV and the event rate is lower. Some of the other cuts may be able to increase the signal to background ratio somewhat, nevertheless, it is difficult to be optimistic about the observability of this LN mode. This conclusion is independent of the mass of the N.

Turning now to the final state L^+L^-, it clearly will produce, after decay, a state of two W's and missing transverse momentum. If both W's decay leptonically, one will see events with two leptons of opposite charge and missing transverse momentum (carried off by $N\overline{N}$ and the neutrinos from the W decays). This is very similar to the state in which the tau was discovered at SPEAR.[13] In this channel the dominant background arises from W^+W^- events which can also give rise to two charged leptons and missing transverse momentum.

However, we show in Fig. 5 that if the event is projected into the transverse plane and the distribution in angle (ϕ) between the two leptons examined it will be found that there is a range over which the signal exceeds the background. Notice that $\phi = 0$ corresponds to the back-to-back configuration. In this plot we have included the

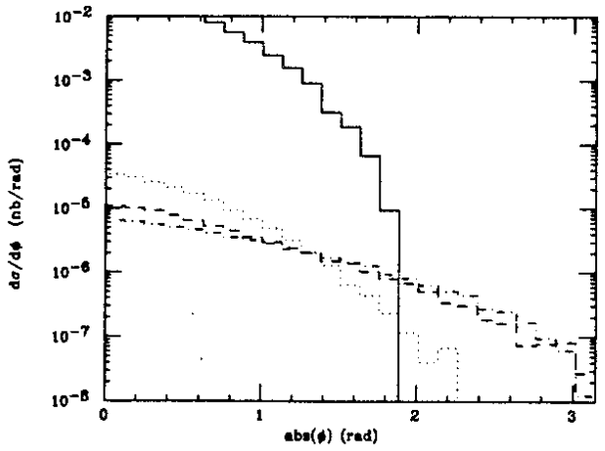

Figure 5. The distribution in the variable ϕ defined as the absolute value of the difference in the azimuthal angle of the two charged leptons resulting from the process $pp \to L^+L^- + X \to l^+l^-N\overline{N}\nu\overline{\nu}+X$ at $\sqrt{s} = 40$ TeV. N is taken to be massless. The charged leptons (l) which can be either e or μ are required to satisfy $p_t > 50$ GeV and $|y| < 3$. The dotted, dashed and dot-dashed histograms correspond to m_L=100, 200 and 400 GeV. The solid histogram is the background arising from $pp \to WW + X \to l^+l^-\nu\overline{\nu} + X$

decay channels $W \to e\nu$ and $W \to \mu\nu$ and have required that the charged leptons have $p_t > 50$ GeV and $|y| < 3$ and have assumed $\sqrt{s} = 40$ TeV. Requiring $|\phi| > 2$ results in approximately 3 signal events and no background in the case of $m_L = 400$ GeV assuming the canonical SSC integrated luminosity of $10^{40}cm^{-2}$. Several comments are in order.

The cut on ϕ becomes more effective at larger values of m_L, since the charged leptons become less tightly correlated than those in the background. Indeed, it is probably not possible to detect a heavy lepton of mass below 120 GeV by this method. There is an additional source of background from the W pairs arising from the production and decay ($b' \to Wt$) of a pair of fourth generation quarks,* and also from the production of top quarks if the top quark is heavier than the W. These events occur at a much larger rate than the production of W pairs (provided $m_{b'} < 600$ GeV)) but have more jets (from the t and $\overline{t}$) in them; they must be rejected by requiring the absence of such jets. There is a possible background arising from the final state of $ZZ^* \to \nu\overline{\nu}e^+e^-$, where Z^* indicates an off-shell Z boson. This background, if relevant, can be eliminated by looking at $e\mu$ final states.

The number of events passing the cuts is small and the detection of a heavy lepton by this method is limited by the available integrated luminosity rather than by the background. If experiments are possible at higher integrated luminosities or the Higgs mass is larger so that the event rate is increased (see Fig. 3) then this mode is exploitable. At $\sqrt{s} = 17$ TeV the rate is lower by a factor of 4 or so and the signal correspondingly more difficult to extract.

The event rate is larger if one of the W's is detected via its hadronic decay modes. In this case the signal consists of an isolated lepton and some hadronic jets whose invariant mass reconstructs to the W mass. One background arises from W pairs as before. But now there is a potentially much larger source – the final state $W + jets$ where the $jets$ system has invariant mass near the W mass and is indistinguishable from the jets from a real W decay.

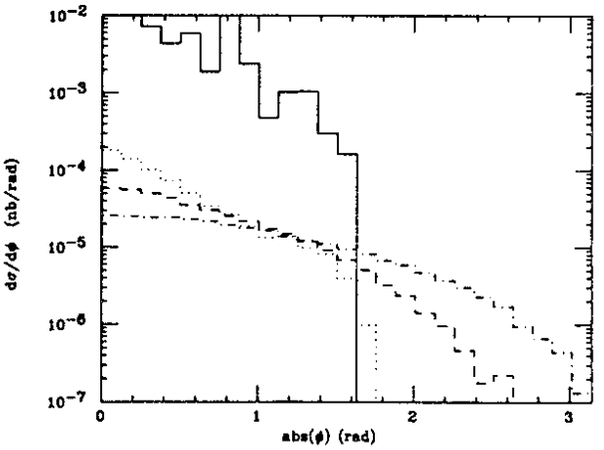

Figure 6. The distribution in the variable ϕ defined as the absolute value of the difference in the azimuthal angle of the charged leptons and the hadronic system from the W resulting from the process $pp \to L^+L^- + X \to l^\pm W^\mp(\to hadrons)N\overline{N}\nu + X$ at $\sqrt{s} = 40$ TeV. N is taken to be massless. The charged lepton (l) which can be either e or μ is required to satisfy $p_t > 20$ GeV and $|y| < 3$. The W is decayed to $q\overline{q}$ and the following cuts on the rapidity (y), transverse momentum and azimuthal angle (ϕ_q) of the quark and antiquark made: $|y| < 5$, $p_t > 50$ GeV, $\sqrt{((\phi_q - \phi_{\overline{q}})^2 + (y_q - y_{\overline{q}})^2)} > 0.5$. The dotted, dashed and dot-dashed histograms correspond to m_L=100,200 and 400 GeV. The solid histogram is the background arising from $pp \to W + jets + X \to l^\pm\overline{\nu} + jets + X$. The two parton system is subject to the same cuts as the quark and antiquark in the signal, In addition the invariant mass of the system must be in the range $M_W \pm 20$ GeV.

Figure 6 shows the distribution in the angle ϕ in the transverse plane between the lepton and the vector formed by the jet system. At the parton level the background consists of 2 jets which are here required to have an invariant mass of $M_W \pm 20$ GeV. The background is severe but again a cut on ϕ can reject it. A cut requiring that $|\phi| > 1.7$ rejects all the background.** For $m_L = 400$

* We are assuming that the charge 1/3 member (b') of the quark doublet is the lighter.

** The background from W pair events is also eliminated by this cut.

GeV, 70 signal events remain at $\sqrt{s} = 40$ TeV for an integrated luminosity of $10^{40} cm^{-2}$. The rate is about a factor of 4 less at $\sqrt{s} = 17$ TeV. Notice that it is not necessary to measure the missing transverse momentum in the event, and an additional cut on the missing transverse momentum is not useful.

If there exists a new W or Z boson then the production rates for a heavy lepton will rise. As an example consider the case of a new W boson of mass 1 TeV (400 GeV) with the same coupling strength to quarks and leptons as the standard model W (it could, for example, be one occurring in a left-right symmetric model). The production cross-section[1] at SSC is of order 0.1 nb (1.5 nb). The branching ratio into LN will be approximately

$$6\%\sqrt{1+a^2+b^2-2(a+b+ab)}(1-a/2-b/2-(a-b)^2/2))$$

where $a = m_L^2/m_W^2$ and $b = m_N^2/m_W^2$. It is clear therefore that the rate of LN production from new W's of mass 1 TeV is *less* than that from the quark-antiquark annihilation process shown in Fig. 3. In the case of a 400 GeV new W and an L of mass 300 GeV (N is massless), the rate for LN production is *increased* by about a factor of 15. This increase may not be sufficient to overcome the large backgrounds in this channel.

The signals are much more complicated if the N decays inside the detector. The N can decay via its mixing with other neutrinos (separate lepton number conservation for each generation is violated). The possible decays are $N \to l^+ l^- \nu$ where l is any other charged lepton (l^+ and l^- could be τ^+ and μ^- for example). In this case detection will be much easier since the event will have additional charged leptons. The LN final state will produce 4 leptons and a W; a signal which will stand clearly above backgrounds.

2.3. Heavy Lepton Summary

The discussion in this paper has been at the parton level only. A fully convincing demonstration of a signal is only possible with the use of a full Monte-carlo event generator and a detector simulation. Since one of the backgrounds involves jets and W's, such a generator needs to have this final state as one of its options. This final state is only implemented in leading-log approximation in current event generators.[14] This approximation may only be accurate to a factor of three or so. The effectiveness of cuts involving leptons used to establish a signal are very unlikely to be compromised by a full simulation. The cuts on the jet system are more problematic but are not very stringent; the main issue is how well the reconstructed jet direction follows that of the partons which initiate the jet.

In conclusion, it has been demonstrated in this work by I. Hinchliffe that it is possible to devise a set of cuts whereby a 4^{th} generation charged lepton in a doublet with a stable neutrino could be detected in a hadron collider. The detection is limited by event rate and hence the highest energy and integrated luminosity is needed. In the event that the neutrino is unstable and decays within the detector, there are no relevant standard model backgrounds and a signal can be seen.

2.4. Heavy Lepton Appendix

The cross-sections for the relevant production processes are given here. s is the total center of mass energy squared of the initial partonic system. There are two contributions from the gluon-gluon initial state which add incoherently. Firstly from Fig. 2 where the intermediate particle is a Z.

$$\sigma(gg \to L^+L^-) = \frac{\beta\alpha^2\alpha_s^2}{2048\pi \sin^4\theta_W} \frac{m_L^2}{m_W^4}|I|^2$$

where $\beta = \sqrt{1-4m_L^2/s}$, α and α_s are the electromagnetic and strong coupling constants and θ_W is the weak mixing angle. Also

$$I = 2\sum_Q (\pm) \int_0^1 dx \int_0^{1-x} dy \frac{xy}{xy - m_Q^2/s}$$

The sum runs over all quarks of mass m_Q. The + (-) sign applies to charge 2/3 (-1/3) quarks. If the intermediate particle is a Higgs boson

$$\sigma(gg \to L^+L^-) = \frac{\beta^3\alpha^2\alpha_s^2}{4608\pi \sin^4\theta_W} \frac{m_L^2}{m_W^4} \times |J|^2 \frac{s^2}{(s-m_H^2)^2 - \Gamma_H^2 m_H^2}$$

Here m_H (Γ_H) is the mass (width) of the Higgs boson and

$$J = 3\sum_Q \int_0^1 dx \int_0^{1-x} dy \frac{1-4xy}{1-xys/m_Q^2}$$

and again the sum runs over all quark flavors.

Secondly the quark-antiquark initial states give

$$\sigma(q_i\overline{q_i} \to L^+L^-) = \frac{8\pi\alpha^2}{9s} \times \left[\frac{\beta B}{2}\left(e_i^2 - \frac{e_i s(s-m_Z^2)(L_q+R_q)(L_e+R_e)}{8\sin^2\theta_W\cos^2\theta_W((s-m_Z^2)^2+\Gamma_Z^2 m_Z^2)}\right) + \frac{\beta s^2(L_e^2+R_e^2)[B(L_Q+R_Q)^2+2\beta^2(L_Q-R_Q)^2]}{256\sin^4\theta_W\cos^4\theta_W((s-m_Z^2)^2+\Gamma_Z^2 m_Z^2)}\right]$$

where $B \equiv 3-\beta^2$, e_i is the charge of the quark of type i, $L_e = 2\sin^2\theta_W - 1$, $R_e = 2\sin^2\theta_W$, $L_q = \tau_3 - 2e_i\sin^2\theta_W$

and $R_q = -2e_i \sin^2\theta_W$ with $\tau_3 = 1(-1)$ if $e_i = 2/3(-1/3)$.

$$\sigma(u\bar{d} \to L^+N) = \frac{\pi\alpha^2|U_{ud}|^2}{48\sin^4\theta_W} \frac{\beta s}{(s-m_W^2)^2 - \Gamma_W^2 m_W^2} \times \left(1 + \frac{\beta^2}{3} - \left(\frac{m_L^2 - m_N^2}{s}\right)^2\right).$$

Here U is the appropriate element of the Kobayashi-Maskawa matrix and in this equation

$$\beta = \left(1 - 2\frac{m_L^2 + m_N^2}{s} + \left(\frac{m_L^2 - m_N^2}{s}\right)^2\right)^{1/2}$$

3. Heavy W' and Z' Bosons

3.1. Heavy Bosons Introduction

In this chapter we summarize the potential discovery limits for new heavy bosons ($W'^{\pm}$ and Z'^0) at the SSC and at an upgraded Tevatron Collider. We consider the production of heavy gauge bosons within classic Left-Right (LR) Symmetric gauge models[15] and within the context of E_6 superstring-inspired models. We also address the question of whether there is sufficient information available at hadron colliders to uniquely determine the couplings of Z' bosons and to distinguish between the various models. In all cases we are considering the production of heavy gauge bosons and their subsequent decays into lepton pairs. More precisely, we focus on the processes

$$\begin{Bmatrix} pp \\ p\bar{p} \end{Bmatrix} \to \begin{Bmatrix} Z'^0 \to e^+e^- \\ W'^{\pm} \to e^{\pm}\nu_R \end{Bmatrix}.$$

or into modes with muons.

The results are clearly model dependent since the couplings and branching ratios are fixed only in the context of various assumptions. The work reported in the next subsection on the classic Left-Right models was done by Grifols, Mendez and Barnett, while the E_6 inspired work (which also includes Left-Right models) was done by Hewett and Rizzo. It is important to note that the two groups used different benchmarks for discovery limits. The first group required 5 events (per year for design luminosity) in the e^+e^- mode while the second group required 5 events in either the e^+e^- or $\mu^+\mu^-$ mode (i.e.- the first group required twice as many events as the second). For SSC the yearly integrated luminosity as taken to be 10^4 pb^{-1} whereas it was 100, 1000 and 30 pb^{-1} for Tevatron upgrades A, B and C (see Chapter I).

3.2. Heavy Bosons from Left-Right Models

To be specific we chose a particular model[15] in which the vertex $Z'ff$ is given by: $g\gamma_\mu(G_L P_L + G_R P_R)$ where $P_L = (1-\gamma_5)/2$, $P_R = (1+\gamma_5)/2$ and where

$$\begin{aligned}
G_L(Z'uu) &= -C\sin^2\theta_W/6 \\
G_R(Z'uu) &= -C(7\sin^2\theta_W - 3)/6 \\
G_L(Z'dd) &= -C\sin^2\theta_W/6 \\
G_R(Z'dd) &= C(5\sin^2\theta_W - 3)/6 \\
G_L(Z'ee) &= C\sin^2\theta_W/2 \\
G_R(Z'ee) &= C(3\sin^2\theta_W - 1)/2 \\
G_L(Z'\nu\nu) &= C\sin^2\theta_W/2 \\
G_R(Z'\nu\nu) &= -C(\sin^2\theta_W - 1)/2
\end{aligned}$$

where $C \equiv 1/(\cos\theta_W(\cos 2\theta_W)^{\frac{1}{2}})$. In this model assuming three light generations including the right-handed neutrino ν_R, the width of the new boson is $\Gamma_{Z'} = \alpha C^2 M_{Z'}(1 - 4\sin^2\theta_W + \frac{14}{3}\sin^4\theta_W)/\sin^2\theta_W$ (using $g^2 = 4\pi\alpha/\sin^2\theta_W$).

To evaluate the branching ratios of the Z' we note that the possible decay channels are $e_i^+e_i^-$, $\nu_i\bar{\nu}_i$, $u_i\bar{u}_i$, $d_i\bar{d}_i$, W^+W^- and ZH, where $i = 1,2,3$ is a generation index and H is the light "standard" Higgs boson of the LR models. In the usual LR model with a scalar sector consisting of one bidoublet and two triplets, the last two channels are always allowed and it can be shown[16] that the mixing $Z_L - Z_R$ (which is fixed by the masses and is very small) leads to $BR(Z' \to WW) \approx BR(Z' \to e^+ + e^-)$. On the contrary, the mixing between W_L and W_R can vary from zero to some upper bound depending on the relative values of the bidoublet vev's κ and κ'. In fact the zero value for the mixing (corresponding to $\kappa' = 0$) is required phenomenologically.[17] For the W' the possible decay channels then are $e_i\bar{\nu}_{Ri}$ and $d_i\bar{u}_i$ (*i.e.*- we do not consider the channels WZ and WH since they would only be allowed if the $W_L - W_R$ mixing were not zero).

The total width is obtained by summing over the partial widths of all these channels.[16] The branching ratios of interest are then

$$BR(Z'^0 \to e^+e^-) = 1.8\%\,, \quad BR(W'^{\pm} \to e^{\pm}\nu_R) = 8\%\,.$$

The exclusion of the WW and ZH channels would increase $BR(Z' \to e^+e^-)$ from 1.8 to 1.9%. If ν_R is very heavy, then the branching ratio would be increased to 2.3%.

The production rates are shown in Figs. 7 and 8 for different upgrade options of the Tevatron. For reference, the corresponding rates for the SSC are shown in Fig. 9. The rapidity cuts are introduced in the initial quark-antiquark system. Figure 10 shows the sensitivity of the cross sections to the rapidity cut for the SSC case.

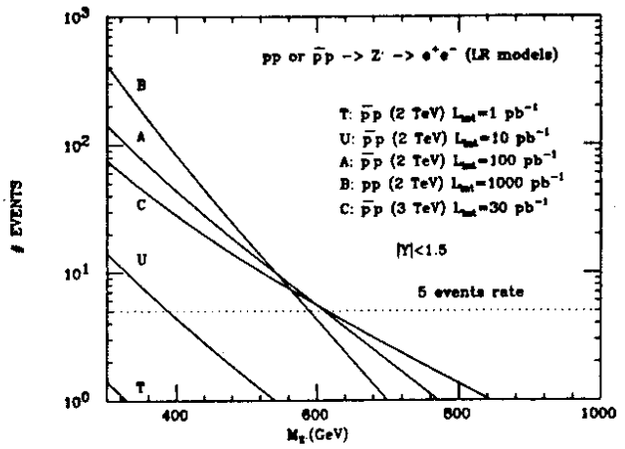

Figure 7. The production rates for Z'^0 from the model of Ref. 15 at the Tevatron Collider.

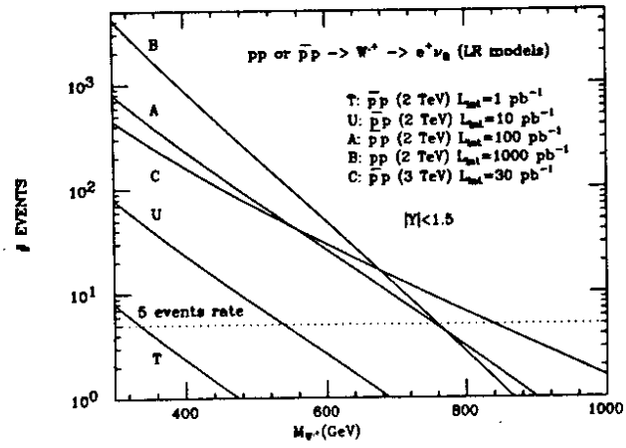

Figure 8. The production rates for W'^+ from the model of Ref. 15at the Tevatron Collider. Note that all rates are the same for W'^- for $p\bar{p}$ colliders, but that the rates for W'^- are a factor of about two lower at pp machines.

3.3. Heavy Bosons from E_6 Inspired Models

Interest in the possibility of observing new neutral gauge bosons at hadron colliders has been renewed due to the advent of E_6 superstring-inspired models.[18] In our work below we will concentrate our discussion on two classes of models originating from E_6:

$$\begin{aligned} &\text{(A)} \quad \mathrm{SU(3)}_C \times \mathrm{SU(2)}_L \times \mathrm{U(1)}_Y \times \mathrm{U(1)}_\theta \\ &\text{(B)} \quad \mathrm{SU(3)}_C \times \mathrm{SU(2)}_L \times \mathrm{SU(2)}_R \times \mathrm{U(1)} \end{aligned} \tag{1}$$

Models of type (A) are the so-called 'effective rank-5' models (ER5M) which contain a free parameter (θ) describing the amount of mixing between the Z_ψ and Z_χ states (from the decomposition $E_6 \to \mathrm{SO(10)} \times \mathrm{U(1)}_\psi \to \mathrm{SU(5)} \times \mathrm{U(1)}_\chi \times \mathrm{U(1)}_\psi$) within the Z'. If the mixing between the Z' and standard model (SM) Z is ignored, then

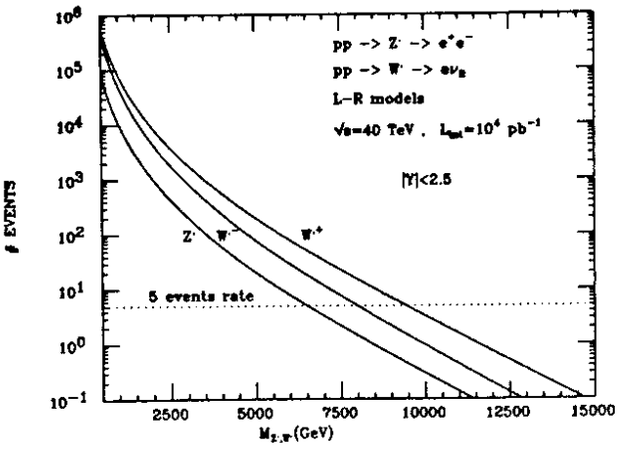

Figure 9. The production rates for Z'^0 and $W'^\pm$ from the model of Ref. 15 at the SSC.

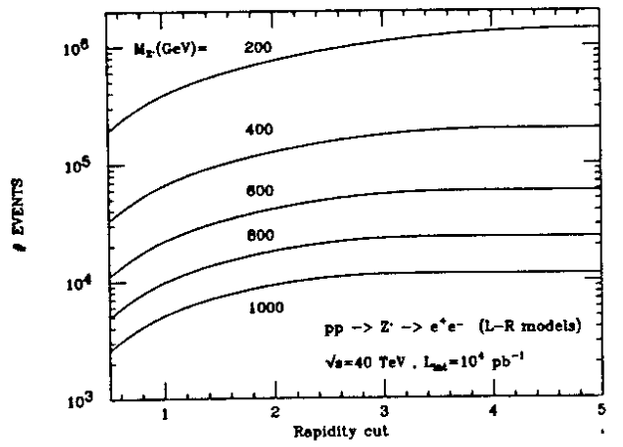

Figure 10. The dependence on the rapidity cut of the production rates for Z'^0 from the model of Ref. 15 at the SSC.

Z' is a mass eigenstate; this is an excellent approximation in general when the Z' mass is $\gtrsim 0.4$ TeV or so, which is the case of interest to us here. Models of type (B) are represented by the usual left-right model[19] (LRM) as well as the alternative left-right model[20] (ALRM). The LRM and ALRM are quite distinct in that their associated Z' bosons have very different couplings and that the right-handed charged gauge boson (W_R) can be light ($\simeq 210$ GeV) in the ALRM whereas it is expected to be heavy ($\gtrsim 2$ TeV) in the LRM. W_R in the ALRM also carries lepton number and negative R-parity so that it cannot be produced by a Drell-Yan-like process at hadron colliders.

In what follows we will address the following questions: (i) what are the search limits for Z' bosons in the various models at hadron colliders and can we distinguish between these models? (ii) Given the unusual nature of the W_R in the ALRM, what search limits can we find for its production? All relevant formulae can be found

elsewhere.[18] In setting detailed search limits on the Z' we will assume a minimum of $N = 5$ events in the $\ell^+\ell^-$ channel (where ℓ can be either e or μ). We will later comment on how our results change when a discovery limit of 10 events in this channel is assumed. These search limits will be quite model dependent since the rate for $p\bar{p}^{(-)} \to Z'^0 \to \ell^+\ell^-$ depends on the quark couplings to the Z' as well as its leptonic branching fraction (B) and these $Z'f\bar{f}$ couplings are dependent on the parameter θ in the ER5M. Even within a given model, this number may vary depending on, *e.g.*, whether exotic fermions in the E_6 **27**-representation can contribute ($n_g = 3$) or not ($n_g = 0$) to the Z' total width.

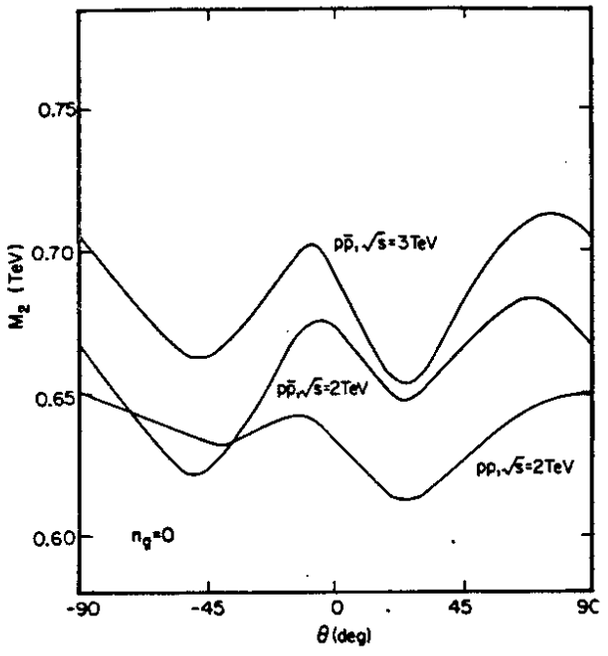

Figure 11. Z' mass limits for the ER5M as a function of θ for the Tevatron uprades assuming $n_g = 0$ and $N = 5$ events.

Figure 11 and 12 show the search limits for the Z' in the ER5M as a function of θ, assuming $N = 5$ and $n_g = 0$, at the Tevatron upgrades and the SSC, respectively. Only the range $-90° \leq \theta \leq 90°$ is shown since mapping $\theta \to \theta + 180°$ leaves the search limits invariant because it merely flips the sign of all Z' couplings. Thus, without Z-Z' mixing, this ambiguity in θ will always remain. The corresponding limits for the Z' in the LRM and the ALRM can be found in Table 1. The figures and the table show the trade-off between machine energy and luminosity as well as *pp vs.* $p\bar{p}$ at the Tevatron. Note that much stronger limits are obtained for both the LRM and ALRM since the overall strength of the couplings is greater in these two cases than in the ER5M.

How do our Z' search limits change if we give up the assumption of $n_g = 0$ and/or the assumption that $N = 5$

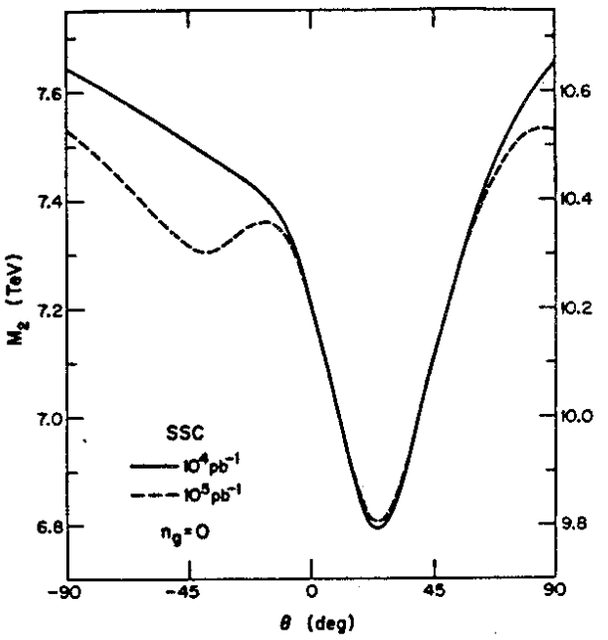

Figure 12. Same as Fig. 1 but for the SSC with $10^4\,\mathrm{pb}^{-1}$ or $10^5\,\mathrm{pb}^{-1}$ integrated luminosity. For 10^4 (10^5) pb^{-1} the left- (right-) hand scale should be used.

events in the $\ell^+\ell^-$ lepton channel? Table 2 shows the limits (or range of limits in the ER5M) for several other values of (n_g, N) for each of the models under consideration. Note that these limits are significantly weaker for every model in comparison to the $n_g = 0$, $N = 5$ case already discussed. When combined with the $n_g = 0$, $N = 5$ case previously discussed, the results in the table generally show the variation one can expect in Z' limits at various hadron colliders within the E_6 model context.

Once produced, are these Z' bosons identifiable, *i.e.*, can we distinguish a Z' originating in the LRM or ALRM from one coming from the ER5M? Can we determine the angle θ uniquely? Certainly, in order to make a detailed study of the Z' boson's properties one needs several hundred to a thousand events and, hence, the Z' must be far lighter than the search limits discussed above. If $n_g = 0$, the only Z' properties useful in determining the couplings are the leptonic branching fraction (B_ℓ), the forward-backward asymmetry for leptons, A_{FB}^{ℓ},[21] and, to a lesser extent, the total Z' width, Γ_0. A measurement of Γ_0 cannot be done very accurately at hadron colliders due to the large energy resolution inherent in such machines. Hadronic Z' decay modes will be invisible due to the large QCD background and will hence be useless in determining the model.

Table 1 and Fig. 13 show the values of A_{FB}^{ℓ} for the various models under consideration for particular values of the Z' mass. Note that in the scaling limit A_{FB}^{ℓ} is $M_{Z'}$ and $\sqrt{s}$ *independent* so that A_{FB}^{ℓ} is not expected to

Table 1

Z' search limits and A_{FB}^{ℓ} values in the LRM and ALRM for the various hadron colliders. In calculating A_{FB}^{ℓ} we take $M_{Z'}(= M_2)$ to be 0.450 TeV (3 TeV) for the Tevatron (SSC). $N = 5$ events and $n_g = 0$ are assumed. Z' masses are in units of TeV.

Machine		$\mathcal{L}$	Z' limit		A_{FB}^{ℓ} limit	
			LRM	ALRM	LRM	ALRM
pp	$\sqrt{s} = 2$ TeV	$10^3\,\text{pb}^{-1}$	0.70	0.76	0.123	−0.230
$p\bar{p}$	$\sqrt{s} = 2$ TeV	$10^2\,\text{pb}^{-1}$	0.75	0.87	0.205	−0.351
$p\bar{p}$	$\sqrt{s} = 3$ TeV	$30\,\text{pb}^{-1}$	0.81	0.97	0.199	−0.344
	SSC	$10^4\,\text{pb}^{-1}$	8.30	9.40	0.103	−0.205
	SSC′	$10^5\,\text{pb}^{-1}$	11.35	12.55	0.103	−0.205

Table 2

Z' search limits in the ER5M, LRM, and ALRM for $n_g = 3$ with $N = 5$, 10 events and for $n_g = 0$ with $N = 10$ events in the $\ell^+\ell^-$ channel ($\ell = e, \mu$) for various hadron colliders. The Z' masses are in units of TeV.

Machine		Model	$N = 5$ $n_g = 3$	$N = 10$ $n_g = 0$	$N = 10$ $n_g = 3$
$p\bar{p}$	(2 TeV)	ER5M	0.52-0.64	0.58-0.66	0.45-0.57
$p\bar{p}$	(2 TeV)	LRM	0.69	0.68	0.61
$p\bar{p}$	(2 TeV)	ALRM	0.76	0.80	0.69
$p\bar{p}$	(3 TeV)	ER5M	0.48-0.66	0.60-0.68	0.40-0.57
$p\bar{p}$	(3 TeV)	LRM	0.71	0.71	0.62
$p\bar{p}$	(3 TeV)	ALRM	0.81	0.86	0.70
pp	(2 TeV)	ER5M	0.53-0.63	0.59-0.63	0.48-0.58
pp	(2 TeV)	LRM	0.65	0.65	0.60
pp	(2 TeV)	ALRM	0.69	0.71	0.64
	SSC	ER5M	5.35-7.20	6.35-7.20	5.05-6.35
	SSC	LRM	7.50	7.40	6.65
	SSC	ALRM	8.05	8.45	7.15
	SSC′	ER5M	8.15-10.05	9.30-9.50	7.25-9.20
	SSC′	LRM	10.45	10.40	9.50
	SSC′	ALRM	11.15	11.60	10.20

be very sensitive to changes in beam energy or the actual value of $M_{Z'}$. It is clear that a B_ℓ measurement, however

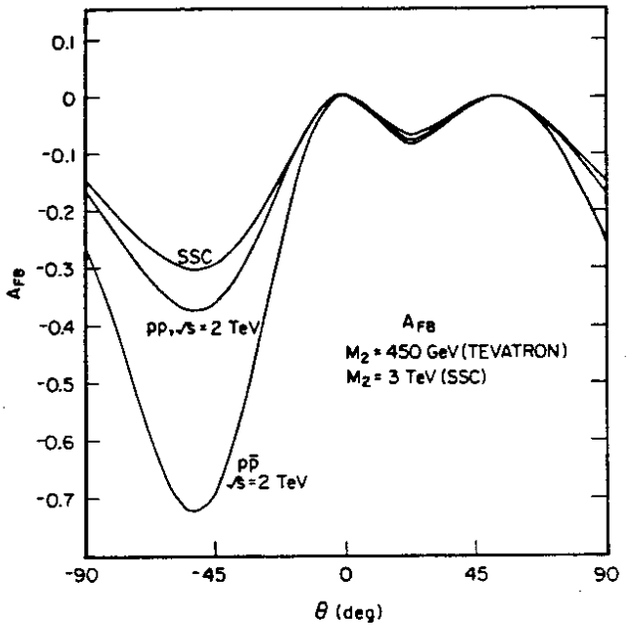

Figure 13. A_{FB}^{ℓ} as a function of θ in the ER5M for the SSC and Tevatron upgrades with $M_Z = 3$ TeV and 450 GeV, respectively.

precise, cannot be used to discriminate between models without an accurate knowledge of Γ_0. The value of A_{FB}^{ℓ} can be used to separate the ALRM and LRM but not the ALRM from the ER5M. The reason for this is that there always exists a value of θ in the ER5M for which $A_{FB}^{\ell}(\text{ER5M}) = A_{FB}^{\ell}(\text{ALRM})$ as can be easily seen from Fig. 13 and Table 1. Thus the sign of A_{FB}^{ℓ} will separate the LRM from the other two models under consideration but will not distinguish the ALRM and the ER5M.

This situation improves somewhat for $n_g = 3$ since there are now additional, unstable, color singlet final states (exotics) accessible in Z' decay for which the QCD backgrounds are quite small. Although the Z' width in this case, Γ_3, would still be only poorly determined, the *relative* branching fractions between these exotic modes and $\ell^+\ell^-$ are Γ_3 independent and could be used to identify the model, at least in principle. If the exotic fermion masses could be determined (by reconstruction) and various exotics separated by their decay final states, then the LRM, ALRM, and ER5M could be easily distinguished and, when combined with A_{FB}^{ℓ} data, can be used to determine θ almost uniquely. The problems with this approach are that the decay modes of these exotics are very dependent on their quantum numbers (baryon and lepton numbers as well as R-parity) assignments, of which there are several possibilities, and that many of the exotics have similar decay patterns. In addition, for many assignments of these quantum numbers, there will be missing energy in the decay final state of these exotics making accurate reconstruction of their masses somewhat difficult. Still, this procedure may hold some promise in determining the

couplings of the new Z' boson.

We now turn to W_R search limits in the ALRM. Due to the usual properties of the W_R discussed above it cannot be produced in the usual manner (*i.e.*, by quark-antiquark annihilation). The best mechanism for W_R production has been found to be[20] gluon$+\overset{(-)}{u} \to W_R^+(W_R^-)+\overset{(-)}{h}$ where h is an exotic fermion with leptoquark quantum numbers and negative R-parity contained in the E_6 **27** representation. Since W_R and h get their masses from the same vev one might expect them to have masses of comparable magnitude. In setting our limits, we have assumed the production of 10 $W_R^{\pm}\overset{(-)}{h}$ events and the details of the production signal have been discussed by Gunion *et al.* in Ref. 20. Table 3 shows a summary of these results. Note that our limits are roughly dependent on the sum of the W_R mass (M_R) and the exotic h fermion mass (m_h). Note also that the sum of the W_R^+h and $W_R^-\overline{h}$ cross sections is the same at pp and $p\overline{p}$ machines so that $\sqrt{s}$ and machine luminosity are the only relevant factors (and not the parton luminosities) in determining these search limits. Also, if $M_R \simeq m_h$ then W_R production may be unobservable at the $p\overline{p}$ Tevatron upgrades since $M_R \gtrsim 210$ GeV from already existing data (see Barger *et al.* in Ref. 20). To really explore a reasonable W_R search range it is clear that the SSC is required.

Table 3

Search limits for $W_R^{\pm}(\overline{h})$ production in the ALRM at various hadron colliders.

	Machine	$\mathcal{L}$	$M_R + m_h$ Search limit
$p\overline{p}$	$\sqrt{s} = 2$ TeV	10^2 pb^{-1}	0.375-0.400 TeV
$p\overline{p}$	$\sqrt{s} = 3$ TeV	30 pb^{-1}	0.405-0.440 TeV
pp	$\sqrt{s} = 2$ TeV	10^3 pb^{-1}	0.500-0.525 TeV
	SSC	10^4 pb^{-1}	4.8-5.6 TeV
	SSC′	10^5 pb^{-1}	6.2-7.4 TeV

It is quite clear that hadron colliders offer a unique opportunity to explore a large mass range in the search for the new gauge bosons expected in E_6 superstring-inspired models.

4. Searches for Supersymmetric Particles

4.1. Supersymmetric Particles Introduction

Supersymmetry is an attractive possible extension of the Standard Model both because of its mathematical elegance and because it provides a natural mechanism for keeping Higgs bosons light even in the presence of a superheavy mass scale such as a grand unification scale or the Planck scale. It has therefore been extensively studied both for existing and for future colliders. The best experimental limits on the masses of gluinos ($\widetilde{g}$) and squarks ($\widetilde{q}$) come from the UA1 Collaboration[22] at the S$\overline{\text{p}}$pS and the CDF Collaboration[23] at the Tevatron. Based on studies of events with jets and substantial missing transverse energy (E_T^{miss}), they find the following limits (independent of the other mass)

$$\begin{aligned} &M_{\widetilde{g}} > 53\,\text{GeV}, \quad M_{\widetilde{q}} > 45\,\text{GeV} \qquad \text{(UA1)} \\ &M_{\widetilde{g}} > 73\,\text{GeV}, \quad M_{\widetilde{q}} > 74\,\text{GeV} \qquad \text{(CDF)} \end{aligned} \tag{4.1}$$

The work reported here was done in the context of the minimal supersymmetric model.[24] To give masses to up and down quarks in this model, it is necessary to introduce two Higgs doublets, resulting in three neutral and one charged pair of Higgs bosons after symmetry breaking. The supersymmetric partners of the Higgs bosons mix with the $\widetilde{\gamma}$ and $\widetilde{Z}$ to make four Majorana states $\widetilde{\chi}_i^0$, $i = 1,2,3,4$, which are known collectively as neutralinos and are numbered in order of increasing mass. Similarly the supersymmetric partner of the charged Higgs boson mixes with the $\widetilde{W}$ to make two chargino states $\widetilde{\chi}_i^+$, $i = 1,2$. We shall assume that R parity is conserved so that all supersymmetric particles are produced in pairs; each supersymmetric particle then decays into lighter supersymmetric particles, and the cascade continues until the LSP ($\widetilde{\chi}_1^0$) is produced which is absolutely stable. This particle escapes from any collider detector.

In the minimal model all of the masses and mixings of the charginos and neutralinos are determined in terms of four parameters. One of these can be eliminated by assuming that the gaugino masses are degenerate at the grand unification or Planck scale. The remaining three parameters can be taken to be the gluino mass $M_{\widetilde{g}}$, a supersymmetric Higgs mass μ, and a ratio $\tan\beta = v_2/v_1$ of Higgs vacuum expectation values (where v_2 (v_1) is the vacuum expectation value of the Higgs that gives mass to the up (down) quarks. If supersymmetry is related to the electroweak scale, we expect both $M_{\widetilde{g}}$ and μ to be less than about 1 TeV; $\tan\beta$ should be of order one. Once the chargino and neutralino mixing angles (and one Higgs mass) are known, the couplings of the mass eigenstates $\widetilde{\chi}_i$ are determined, and all branching ratios can be calculated.

The experimental analyses and most previous Monte Carlo studies[25] have concentrated on the simplest possible decay modes, namely $\tilde{g} \to \tilde{\chi}_1^0 q\bar{q}$ if the gluino is lighter than the squark, or $\tilde{q} \to \tilde{\chi}_1^0 q$ if the squark is lighter than the gluino. They have, furthermore, always assumed that the branching ratios for these direct decays to the LSP are 100%. Since $\tilde{\chi}_1^0$ escapes from the detector, the signature for these modes is large missing transverse energy ($E_T^{\rm miss}$) plus multiple jets. For masses up to $60 - 70\,{\rm GeV}$, these simple modes are dominant for most but not all values of the parameters, so that the current limits (above) are likely to be valid.

However, this assumption begins to break down[26,27] for squark and gluino masses $M_{\tilde{g},\tilde{q}} \gtrsim 100\ GeV$. For example,[27] for $M_{\tilde{g}} = 180\ GeV$ (which would be accessible to an upgraded Tevatron), the branching ratio for the gluino to decay directly to the LSP can be no larger than 0.4 (and may be much smaller depending on the choice of supersymmetric parameters). The suppression is even more dramatic for heavier gluinos ($M_{\tilde{g}} \gtrsim 500\ GeV$), where the branching ratio is no greater than 0.14.

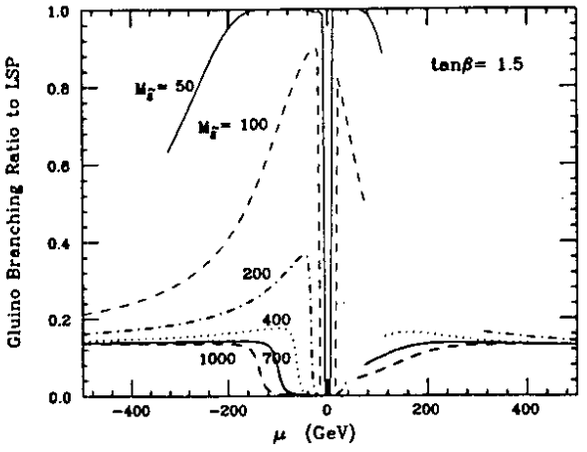

Figure 14. The branching ratio for the direct decay $\tilde{g} \to q\bar{q}LSP$ as a function of the mass of the gluino and the parameter μ.

(See Fig. 14 for the dependence of the branching ratio on various parameters.) This reduction occurs for heavier squarks and gluinos because decays into heavier neutralinos and charginos become possible, and any one mode has a fraction of the total. Even if the details are not correct, this minimal model presumably provides a representative example of supersymmetric models. In more complicated (non-minimal) models such small BR's would also be expected. The heavier neutralinos and chargino states themselves decay, eventually ending up with the LSP.

In general, the decay chains can be rather complicated. In particular, the LSP which eventually gets emitted is much softer and therefore the missing energy signal is degraded. However, the cascade decays can also introduce many interesting new signatures. In particular, it is rather easy to produce leptons in the chain, either via a three body decay of a chargino or neutralino, mediated by the W or Z, or by a direct two-body decay in which the W and Z are produced on-shell and subsequently decay leptonically. We show a particular example of the principal gluino branching ratios at the end of this introductory section.

Thus, it remains an open question whether gluinos can be easily isolated if produced at a future hadron collider. Similar considerations apply to squark production and decay. However the branching ratio suppressions for direct LSP production in squark decay are not as severe, so the "classic" missing energy signature is probably viable. Incidentally, we should emphasize that it is not necessary for *both* gluinos or *both* squarks to decay directly to the LSP in order to obtain large $E_T^{\rm miss}$. In this paper, we concentrate on the more problematic (and more copiously produced) gluinos. Given this, it follows that we should focus on the case for which the squarks are heavier than the gluino (in the opposite case gluinos would have a two-body decay into squarks and it would be more efficient to study the direct squark production). To be definite we often chose $M_{\tilde{q}} = 2M_{\tilde{g}}$ although the precise values of the squark masses have little effect on these results.

The couplings of gluinos to gluons and quarks are completely specified by supersymmetry, and hence the $\tilde{g}\tilde{g}$ production cross section is calculable given the gluino mass (with weaker dependence on squark mass). For $M_{\tilde{g}} = 750\,{\rm GeV}$ at $\sqrt{s} = 40\,{\rm TeV}$ the total $pp \to \tilde{g}\tilde{g}X$ cross section is

$$\sigma_{\tilde{g}\tilde{g}} \simeq 70\,{\rm pb} \tag{4.2}$$

All the decay modes are similarly calculable. For the 750 GeV case the principal gluino branching ratios are (for $m_{H^+} = 500\ GeV$, $\mu = 150\ GeV$ and $\tan\beta = 1.5$)

$$\begin{aligned}
\tilde{g} &\to \tilde{\chi}_1^{\pm} \bar{q} q' \quad 29\% \\
\tilde{g} &\to \tilde{\chi}_2^{\pm} \bar{q} q' \quad 29\% \\
\tilde{g} &\to \tilde{\chi}_1^0 \bar{q} q' \quad 12\% \\
\tilde{g} &\to \tilde{\chi}_2^0 \bar{q} q' \quad 17\% \\
\tilde{g} &\to \tilde{\chi}_4^0 \bar{q} q' \quad 13\%
\end{aligned} \tag{4.3}$$

The chargino branching ratios are

$$\begin{aligned}
\tilde{\chi}_1^+ &\to \tilde{\chi}_1^0 \bar{q} q' \quad 67\% \\
\tilde{\chi}_1^+ &\to \tilde{\chi}_1^0 \ell\nu \quad 33\%
\end{aligned} \tag{4.4}$$

and

$$\begin{aligned}
\tilde{\chi}_2^+ &\to \tilde{\chi}_1^+ Z^0 \quad 41\% \\
\tilde{\chi}_2^+ &\to \tilde{\chi}_1^+ H_2^0 \quad 5\% \\
\tilde{\chi}_2^+ &\to \tilde{\chi}_1^0 W^+ \quad 11\%
\end{aligned}$$

$$\widetilde{\chi}_2^+ \to \widetilde{\chi}_2^0 W^+ \quad 31\%$$
$$\widetilde{\chi}_2^+ \to \widetilde{\chi}_3^0 W^+ \quad 12\% \qquad (4.5)$$

where H_2^0 is the lightest Higgs scalar. The neutralino branching ratios are

$$\widetilde{\chi}_2^0 \to \widetilde{\chi}_1^0 H_2^0 \quad 100\% \qquad (4.6)$$

and

$$\widetilde{\chi}_3^0 \to \widetilde{\chi}_1^0 Z^0 \quad 19\%$$
$$\widetilde{\chi}_3^0 \to \widetilde{\chi}_1^0 H_2^0 \quad 60\%$$
$$\widetilde{\chi}_3^0 \to \widetilde{\chi}_1^\pm \bar{q} q' \quad 14\%$$
$$\widetilde{\chi}_3^0 \to \widetilde{\chi}_1^\pm \ell \nu \quad 7\% \qquad (4.7)$$

and

$$\widetilde{\chi}_4^0 \to \widetilde{\chi}_1^0 H_2^0 \quad 0.3\%$$
$$\widetilde{\chi}_4^0 \to \widetilde{\chi}_2^0 H_2^0 \quad 6\%$$
$$\widetilde{\chi}_4^0 \to \widetilde{\chi}_3^0 Z^0 \quad 8\%$$
$$\widetilde{\chi}_4^0 \to \widetilde{\chi}_1^\pm W^\mp \quad 85\% \qquad (4.8)$$

The work reported in this section was done by many members of the group. This summary is an amalgam from three written contributions submitted by various combinations of H. Baer, R.M. Barnett, J. Freeman, J.F. Gunion, H.E. Haber, R.J. Hollebeek, F.E. Paige, R. Raja, X. Tata, A.P. White, and J. Woodside.

4.2. The Missing-Energy Signature for Gluinos Using a Partonic Monte Carlo with the Full Cascade Decays

In this section (work by Baer, Tata and Woodside) we compute the missing transverse energy signal[28] expected from the process $p\bar{p}$ (or pp) $\to \widetilde{g}\widetilde{g}X \to q\bar{q}\widetilde{\chi}_i + q\bar{q}\widetilde{\chi}_j + X$ where the $\widetilde{\chi}$ collectively denotes the two charginos ($\widetilde{\chi}_{1,2}^\pm$) and the four neutralinos ($\widetilde{\chi}_{1,2,3,4}^0$) of the minimal model. These charginos and neutralinos then decay via the two body modes $\widetilde{\chi}_i \to \widetilde{\chi}_j + (V \text{ or } H)$ (here $V = W^\pm$ or Z, and H is any Higgs scalar) if these are kinematically accessible; otherwise, they decay into a fermion pair (quark or lepton) and a lighter $\widetilde{\chi}$. The secondary $\widetilde{\chi}$ again decays as described above unless it is $\widetilde{\chi}_1^0$, which we take to be the lightest supersymmetric particle, LSP. Thus the final state from $\widetilde{g}\widetilde{g}$ production consists of n quarks + m leptons ($n \geq 4$, $m \geq 0$) + $E_T^{\rm miss}$ (coming from the two $\widetilde{\chi}_1^0$'s and any neutrinos). The relevant branching fractions are computed as specified in Ref. 29, see the example shown above.

Shown in Fig. 15 is the number of gluino pairs expected annually at (A) a 2 TeV $p\bar{p}$ collider with $\int Ldt = 100pb^{-1}$, (B) a 2 TeV pp collider with $\int Ldt = 1000pb^{-1}$, and (C) a 3 TeV $p\bar{p}$ collider with $\int Ldt = 30pb^{-1}$ which are representative of the various options for the upgrading

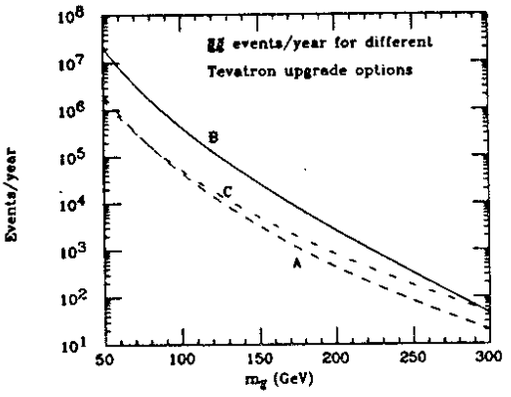

Figure 15. Expected rate of production of $\widetilde{g}\widetilde{g}$ events versus $M_{\widetilde{g}}$ for the three different Tevatron upgrade options discussed in the text. We take $M_{\widetilde{q}} = 2\, M_{\widetilde{g}}$.

to phase II of the Tevatron in the next decade. Here we have taken $M_{\widetilde{q}} = 2\, M_{\widetilde{g}}$. We see from Fig. 15 that option B gives the greatest number of gluino pairs unless $M_{\widetilde{g}} >$ 300 GeV.

In our computation of the various event topologies, we have incorporated the complete decay cascade of the $\widetilde{g}, \widetilde{\chi}_i^\pm$ and $\widetilde{\chi}_i^0$ as given by the minimal supergravity model. Although the gluino production cross-sections do not depend on the parameters $\tan\beta$ (the ratio of Higgs field vev's) and μ, that enter the chargino and neutralino mass matrices, the cross-section into each event topology, in principle, does depend on these parameters via the branching fractions. Except for small values of μ, the cross sections for multijet + 0, 1 or 2 leptons are relatively insensitive to these parameters.

Small positive values of μ are already disallowed as discussed in Ref. 30. For definiteness, we have taken $\mu = -150GeV$, $\tan\beta = 1.5$ and $M_{\widetilde{q}} = 2\, M_{\widetilde{g}}$ as "typical values" in our calculation. In terms of these parameters (and $M_{\widetilde{g}}$) all the cross-sections can be calculated.

Our calculations have been performed at the parton level. We have coalesced two partons within

$$\Delta R(\equiv \sqrt{\Delta\eta^2 + \Delta\varphi^2}) < 0.7$$

into a single jet and have required $\mid \eta_{jet} \mid < 2.5$ and $E_T(jet) > 15$ GeV. We require (for zero-lepton topologies) a trigger $E_T^{\rm miss} > 50$ GeV.

The results of our calculation for n *jet* + $E_T^{\rm miss}$ events at a 2 TeV $p\bar{p}$ collider (option A) are shown in Fig. 16. Dominant standard model backgrounds are listed in Table 4. For brevity, we have not shown the corresponding cross-sections for options B and C discussed above. These can be approximated by scaling the cross-sections in Fig. 16 by a ratio of the production rates that can be obtained from Fig. 15. We have computed the following Standard Model backgrounds to the signals:

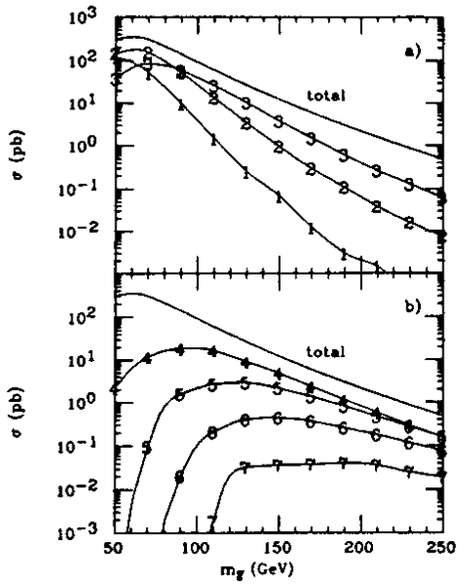

Figure 16. Cross-section for producing n-jet + E_T^{miss} events from gluino pairs versus $M_{\tilde{g}}$ at a 2 TeV $p\bar{p}$ Collider. We take $M_{\tilde{q}} = 2\ M_{\tilde{g}}$, and require $E_T^{miss} > 50$ GeV. Along with the total rate, we show (a) n = 1-3 and (b) n = 4-7 jet topologies.

(*a*) Z + "jets".

(*b*) $W \rightarrow \tau$ + "jets".

(*c*) $t\bar{t}$ production.

Table 4

Background rates from standard model processes for the signals shown in Figure 16. All numbers are in picobarns.

n JETS + E_T^{miss} ($E_T^{miss} > 50$ GeV)

# Jets	Z	W→τ	t(60)	t(120)	Tot.(60)	Tot.(120)
1	23	7	9	.3	39	30
2	11	20	13	.9	44	32
3	3	4	10	1.4	17	8
4	.5	.8	3	1	4	2
5	.02	.06	.2	.2	.3	.3

For the background computation, we used a shower Monte-Carlo described in Ref. 31 for W and Z processes and the same experimental criteria as for the signal. We also computed the background from $t\bar{t}$ production for m_t = 60 and 120 GeV.

The following comments are in order: For $M_{\tilde{g}} \lesssim 120$ GeV, dijets and trijets dominate the signal, while four and five jet events dominate for $M_{\tilde{g}} > 120$ GeV. The dijet (trijet) rate exceeds background for $M_{\tilde{g}} < 90$ (115) GeV, whereas four (five) jet events exceed background for $M_{\tilde{g}}$ < 150 (200) GeV. The large rate for E_T^{miss} events with five or more jets is a direct consequence of allowing for the complete gluino cascade. Running under option B, we would expect about 600 five jet events/year for $M_{\tilde{g}}$ = 200 GeV. We expect that by tuning the cuts to optimize signal/background, option B should easily probe $M_{\tilde{g}}$ = 200 - 250 GeV.

To summarize, from the theorists perspective option B (a Tevatron upgrade to a pp collider operating at $\sqrt{s}$ = 2 TeV and $\int L\ dt = 1000\ pb^{-1}$) gives the highest event rate for gluinos if $M_{\tilde{g}} < 300$ GeV. Backgrounds should be more manageable because of lower W and Z production rates relative to a $p\bar{p}$ collider.

4.3. The Missing-Energy Signature from the Production of $\tilde{\gamma}\tilde{g}$

Here, we focus (following Baer, Tata and Woodside) on the process $pp \rightarrow \tilde{g}\tilde{\chi}_1^0$, where $\tilde{g} \rightarrow q\bar{q}\tilde{\chi}_i^0$, or $q\bar{q}\tilde{\chi}_i^{\pm}$. Production would be signalled by jets in one hemisphere recoiling against a very large E_T^{miss} . As we will see, the E_T^{miss} backgrounds from strong interaction processes within the SM can be eliminated by simple kinematic cuts. This process may, therefore, provide an interesting way to search for relatively light gluinos at the SSC, and, in particular, provide a partial answer to the question, "Is there a window of gluino masses that cannot be explored either at an upgraded Tevatron or the SSC?"

$\tilde{g}\tilde{\chi}_1^0$ production at the SSC proceeds via $q\bar{q}$ annihilation mediated by $\tilde{q}_L$ and $\tilde{q}_R$ exchanges in the t- and u-channels. The production rate, therefore, depends sensitively on $M_{\tilde{q}}$. It also depends on the parameters μ and $\tan\beta$ that enter the $q\tilde{q}\tilde{\chi}_1^0$ couplings via the neutralino mass matrix. We have checked, however, that $\sigma_{\tilde{g}\tilde{\chi}_1^0}$ depends only weakly on μ and $\tan\beta$ except for a small region of parameter space where $\tilde{\chi}_1^0$ is almost a higgsino. For definiteness, we have taken μ = 400 GeV, $\tan\beta = 1.5$ and $M_{\tilde{q}} = 2\ M_{\tilde{g}}$ in our analysis. Except for the "higgsino region" discussed above, $\sigma_{\tilde{g}\tilde{\chi}_1^0} = (6.5 \pm 1.0)$ pb for $M_{\tilde{g}}$ = 220 GeV and $\sigma_{\tilde{g}\tilde{\chi}_1^0} = (2 \pm 0.3\text{pb})$ for $M_{\tilde{g}} = 300$ GeV. These rates are considerably larger (by a factor of 3-4 for $M_{\tilde{q}} = M_{\tilde{g}}$) for lighter squarks. If we assume $M_{\tilde{q}} \simeq 2\ M_{\tilde{g}}$, $\sim$ few $\times 10^4$ $\tilde{g}\tilde{\chi}_1^0$ events are expected annually at the SSC for $M_{\tilde{g}}$ = 200 - 300 GeV, the maximum reach of an upgraded Tevatron.

The E_T^{miss} spectrum from $\tilde{g}\tilde{\chi}_1^0$ production is shown in Fig. 17 for $M_{\tilde{g}} = 220$ GeV. Also shown is the E_T^{miss} spectrum from $\tilde{g}\tilde{g}$ events and from "$Z \rightarrow \nu\bar{\nu}$ + jet(s)" events. In our computation of the supersymmetric processes we have used a parton level Monte Carlo program that incorporates the complete cascade decay of the gluinos and the

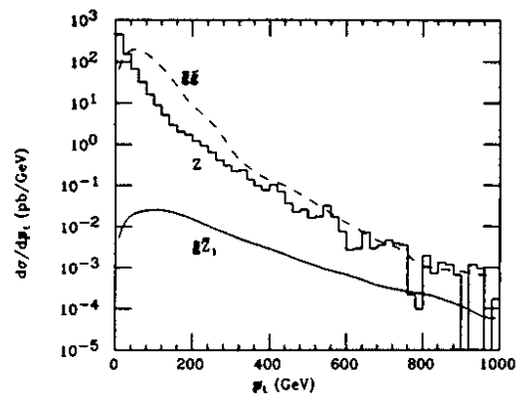

Figure 17. $E_T^{\rm miss}$ spectrum from $\widetilde{g}\widetilde{g}$, $\widetilde{g}\widetilde{\chi}_1^0$, and Z + jets (where $Z \to \nu\nu$) produced in pp collisions at $\sqrt{s} = 40$ TeV. We have taken $M_{\widetilde{g}} = 220$ GeV, $\tan\beta = 1.5$ and $\mu = 400$ GeV.

subsequent $\widetilde{\chi}_i^0$ and $\widetilde{\chi}_i^{\pm}$. The "Z + jet" cross-section has been computed using the shower Monte Carlo program of Ref. 32. We see that $\widetilde{g}\widetilde{\chi}_1^0$ production is completely swamped by the other processes for the whole range of $E_T^{\rm miss}$. In order to isolate the $\widetilde{g}\widetilde{\chi}_1^0$ signal, we have further required that there be no hadronic activity with $E_T >$ 30 GeV outside a 90° cone (in the transverse plane) back to back with the $E_T^{\rm miss}$ vector. We find that this isolation requirement on the $E_T^{\rm miss}$ vector completely cuts out all $\widetilde{g}\widetilde{g}$ events if we also require $E_T^{\rm miss} > 400$ GeV. We expect that this requirement cuts out the $E_T^{\rm miss}$ background from heavy flavour production with even a greater efficiency. The dominant SM background, therefore, comes from $Z \to \nu\overline{\nu}$ + jets.

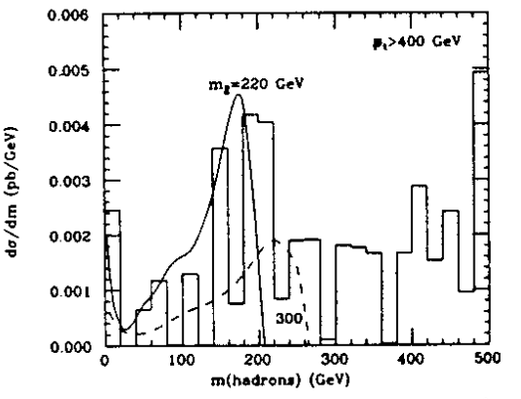

Figure 18. Invariant mass of all hadrons in the transverse hemisphere opposite the $E_T^{\rm miss}$ vector. We require $E_T^{\rm miss} > 400$ GeV and isolation. The histogram is the contribution from Z + jets where $Z \to \nu\overline{\nu}$. The solid line is from $\widetilde{g}\widetilde{\chi}_1^0$ with $M_{\widetilde{g}} = 220$ GeV while the dashed line is for $M_{\widetilde{g}} = 300$ GeV.

The distribution of the invariant mass, m, of the hadronic system for those events with $E_T^{\rm miss} > 400$ GeV and which satisfy the $E_T^{\rm miss}$ isolation requirement is shown in Fig. 18 for $M_{\widetilde{g}} = 220$ and 300 GeV. μ, $\tan\beta$ and $M_{\widetilde{g}}$ are fixed as stated earlier. Also shown is the background distribution from the shower calculation of Z^o + jets, for which we ran 10^6 events, corresponding to 34 CPU hours on a VAX 8700.

About 4000 (2300) $\widetilde{g}\widetilde{\chi}_1^0$ events pass our cuts for $M_{\widetilde{g}}$ = 220 GeV(300 GeV) assuming an integrated luminosity of $10^4 pb^{-1}$. The bulk of the background has $m \geq 300$ GeV so that requiring $m \leq 300$ significantly enhances the signal to background for the case of the relatively light gluinos. We see from Fig. 18 that signal to background $\sim$ unity may be possible, but this should be taken with a grain of salt as there is a considerable uncertainty in our estimate of the background (coming from the fact we are sampling a small tail of the background distribution). We have checked that increasing the $E_T^{\rm miss}$ cut to 600 GeV does not significantly improve the situation.

The conclusions of our analysis are rather pessimistic. The observation of a $\widetilde{g}$ via $\widetilde{g}\widetilde{\chi}_1^0$ production at the SSC is, at best, marginal. If the scalar partners of the fermions are all heavy ($\sim$1 TeV) with only the gluinos light, $\widetilde{g}\widetilde{\chi}_1^0$ production is completely obscured by the Z^0 + jet background. Only in the rather fortuitous case where $M_{\widetilde{q}} \simeq M_{\widetilde{g}}$ can we conclude that the signal is substantially larger than the background. Of course, in this case, one would obtain an additional contribution to the signal from $\widetilde{q}\widetilde{\chi}_1^0$ production.

4.4. The Missing-Energy Signature for Gluinos Using the ISAJET Monte Carlo with the Full Cascade Decays

In this section we report a preliminary study of the $E_T^{\rm miss}$ signature and backgrounds for studying supersymmetry for higher masses at SSC energies (done by Barnett, Freeman, Gunion, Haber, Hollebeek, Paige, Raja and White). In our analysis we have considered only gluino pair production and decay. The main conclusion of our preliminary analysis is that, even with the more complicated decays predicted by the minimal supersymmetric model, the $E_T^{\rm miss}$ signature remains observable. We will refine this result and study additional signatures in a future publication.

To simulate the signatures it is necessary to choose specific parameters. The values of μ and $\tan\beta$ are not very crucial because the branching ratio of the gluino to the LSP depends only weakly on them, although other branching ratios vary somewhat more. We have chosen three gluino masses and three sets of values for the other parameters in the minimal supersymmetric model:

i) $M = 150\,\text{GeV}$, $\mu = -150\,\text{GeV}$, $\tan\beta = 1.5$;
ii) $M = 220\,\text{GeV}$, $\mu = +400\,\text{GeV}$, $\tan\beta = 1.5$;

iii) $M = 750\,\text{GeV}$, $\mu = +150\,\text{GeV}$, $\tan\beta = 1.5$.(4.9)

The first mass may be observable at the present Tevatron; the second might be observed either at an upgraded Tevatron or at the SSC; the third is typical of the SSC mass range. In this section we will discuss only the 750 GeV case in detail. As discussed earlier, we have chosen (for definiteness) $M_{\tilde{q}} = 2M_{\tilde{g}}$ although the precise values of the squark masses have little effect on these results. The relevant branching ratios appear above in Eqs. (4.3)-(4.8).

As discussed in the introduction to this chapter, long chains of cascade decays are possible, giving rise to relatively small E_T^{miss} from the final $\tilde{\chi}_1^0$. But these decays also can produce $W^{\pm}$'s, Z^0's, jets, and leptons, leading to many possible signatures. Here we focus on the missing-energy signature using the ISAJET Monte Carlo program to generate $\tilde{g}\tilde{g}$ events including all the above decay modes. In addition to missing energy we use several additional cuts designed to reflect the fact that the gluinos are produced with $p_T(\tilde{g}) \sim M_{\tilde{g}}$ and $y(\tilde{g}) = \mathcal{O}(1)$, so that the decay products typically have large opening angles in the laboratory frame. We should emphasize that it is not necessary for *both* gluinos to decay directly to the LSP in order to obtain large E_T^{miss} .

The Standard Model background to events involving jets, leptons, and E_T^{miss} comes from the QCD production and semileptonic decay of heavy quarks $Q = c$, b, and t and from the production of $W^{\pm}$ and Z^0 at large p_T. We have also used ISAJET to simulate all of these backgrounds. The largest background for gluinos as for most other processes is the production of heavy quark pairs at high transverse momentum from higher-order processes like

$$g + g \to Q + \overline{Q} + g \qquad (4.10)$$

Such higher-order processes can not be directly included in ISAJET without severe double counting, since they are already produced by the QCD evolution, which approximates all higher-order QCD cross sections by a classical Markov branching process. To generate Eq. (4.10), therefore, it is necessary first to generate a primary hard scattering $gg \to gg$ and then to select events with the branching $g \to \overline{Q}Q$. Since the $gg \to gg$ cross section is 100 times larger than the $gg \to \overline{Q}Q$ one, this is rather slow.

To speed up the generation of the QCD background, we have used a trick developed by M. Della Negra of the UA1 Collaboration. Each primary hard scattering is evolved 10 times, and events not containing heavy quarks are immediately discarded. The rest are each hadronized 10 times, and only events containing the desired leptons or E_T^{miss} from neutrinos are saved. Finally the surviving events were weighted appropriately. We have generated 22,500 accepted QCD background events with $p_T >$ 250 GeV (equivalent to 2.25×10^6 events), 15,000 $W^{\pm}$ and 15,000 Z^0 events with $p_T > 250\,\text{GeV}$, and 2000 signal events.

The most characteristic signature of supersymmetry is missing transverse energy in association with multiple jets. We have concentrated on this signature, leaving to future work the study of signatures involving $W^{\pm} \to \ell^{\pm}\nu$ and $Z^0 \to \ell^+\ell^-$ produced in the gluino cascade decay. To analyse the simulated events, we have used a highly idealized calorimeter with uniform segmentation $\Delta y = \Delta\phi = 0.05$ for $|y| < 6$ and Gaussian energy resolutions

$$\left(\frac{\Delta E}{E}\right)_{\text{e.m.}} = \frac{0.15}{\sqrt{E}}, \qquad \left(\frac{\Delta E}{E}\right)_{\text{had.}} = \frac{0.70}{\sqrt{E}}. \qquad (4.11)$$

In future work we will replace this with the more realistic QFL simulation developed for the CDF Collaboration. Then we found all jets with $p_T > 50\,\text{GeV}$ using a simplified version of the UA1 jet algorithm with a clustering radius $\Delta R = 0.7$.

To select the $M = 750\,\text{GeV}$ gluino signal from the QCD and electroweak backgrounds we impose the following set of cuts:

- The highest jet has $p_T > 300\,\text{GeV}$;
- The missing transverse energy is $E_T^{\text{miss}} > 200\,\text{GeV}$;
- The sphericity S calculated in the transverse plane is $S > 0.2$;

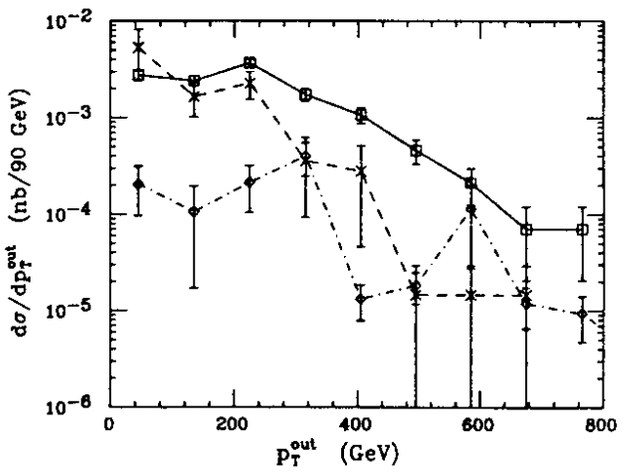

Figure 19. Cross section $d\sigma/dp_T^{\text{out}}$ vs. p_T^{out} after the cuts given in Sec. 4.4. Here p_T^{out} is the missing p_T out of the plane defined by the beam and the highest p_T jet. □ symbol: $\tilde{g}\tilde{g}$ signal. × symbol: QCD background. ◇ symbol: $W^{\pm}$ and Z^0 background. Curves are drawn to guide the eye.

- The number of jets with $p_T > 50\,\text{GeV}$ is $n_{\text{jet}} \geq 4$.

After these cuts we plot the missing transverse momentum p_T^{out} out of the plane defined by the beam and the highest p_T jet. The resulting distribution is shown in

Fig. 19. Making a further cut at $p_T^{\rm out} > 300\,{\rm GeV}$ gives the following cross sections:

$$\sigma_{\rm signal} = 2.4\,{\rm pb}$$
$$\sigma_{QCD} = 0.62\,{\rm pb}$$
$$\sigma_{W^\pm,\,Z^0} = 0.25\,{\rm pb} \qquad (4.12).$$

The signal has been substantially reduced from Eq. (4.2), but it still represents 24,000 events for the nominal integrated luminosity of $10^4\ pb^{-1}$. The signal-to-background ratio seems quite adequate provided that realistic detector effects do not degrade the resolution too much. Presumably the shape of the $p_T^{\rm out}$ distribution could be used to determine the mass, but we have not yet investigated the mass resolution. A detailed study of other gluino signatures will be presented elsewhere.

4.5. Signals from Gluino Decay to Leptons Using a Partonic Monte Carlo with the Full Cascade Decays

We look in this section (following the work of Baer, Tata and Woodside) at the full cascade decays of gluinos and searched for events with energetic, isolated electrons with modest missing energy. As described in a previous subsection (above), we compute the signals[28] expected from the process $p\bar{p}$ (or pp) $\rightarrow \tilde{g}\tilde{g}X \rightarrow q\bar{q}\tilde{\chi}_i + q\bar{q}\tilde{\chi}_j + X$ where the $\tilde{\chi}$ collectively denotes the two charginos ($\tilde{\chi}^\pm_{1,2}$) and the four neutralinos ($\tilde{\chi}^0_{1,2,3,4}$) of the minimal model. These charginos and neutralinos then decay via the two body modes $\tilde{\chi}_i \rightarrow \tilde{\chi}_j$ + (V or H) (here V=W$^\pm$ or Z, and H is any Higgs scalar) if these are kinematically accessible; otherwise, they decay into a fermion pair (quark or lepton) and a lighter $\tilde{\chi}$. The secondary $\tilde{\chi}$ again decays as described above unless it is $\tilde{\chi}^0_1$. Thus the final state from $\tilde{g}\tilde{g}$ production consists of n quarks + m leptons (n $\geq$ 4, m $\geq$ 0) + $E_T^{\rm miss}$ (coming from the two $\tilde{\chi}^0_1$'s and any neutrinos). The relevant branching fractions may be found in Ref. 29. In our computation of the various event topologies, we have incorporated the complete decay cascade of the $\tilde{g}, \tilde{\chi}^\pm_i$ and $\tilde{\chi}^0_i$ as given by the minimal supersymmetry model. For definiteness, we have taken $\mu = -150GeV$, $\tan\beta = 1.5$ and $M_{\tilde{q}} = 2\ M_{\tilde{g}}$ as "typical values" in our calculation. In terms of these parameters (and $M_{\tilde{g}}$) all the cross-sections can be calculated.

Our calculations have been performed at the parton level. We have coalesced two partons within

$$\Delta R(\equiv \sqrt{\Delta\eta^2 + \Delta\varphi^2}) < 0.7$$

into a single jet and have required $\mid \eta_{jet} \mid < 2.5$ and $E_T(jet) > 15$ GeV. For events containing one or more hard ($p_T^\ell > 20$ GeV) and central ($\mid \eta_e \mid < 3$ and $\mid \eta_\mu \mid <$ 0.76) charged leptons, we have used the cut $E_T^{\rm miss} > 20$ GeV. We further require that the leptons be isolated (no partons with $\sum E_T > 3$ GeV in a cone of $\Delta R = 0.4$ about each lepton).

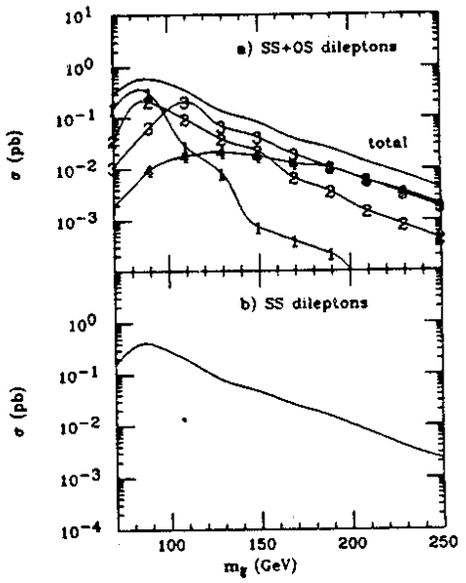

Figure 20. Cross-section for producing isolated dilepton plus n-jet events in $p\bar{p}$ collisions at $\sqrt{s} = 2$ TeV. Cuts are as described in the text. We show (a) all dileptons (summed over $e, \bar{e}, \mu, \bar{\mu}$) and (b) same-sign dilepton rates.

The results of our calculation for n *jet* + 2 *lepton* events at a 2 TeV $p\bar{p}$ collider (option A) are shown in Fig. 20. Dominant standard model backgrounds are listed in Table 5. For brevity, we have not shown the corresponding cross-sections for options B and C discussed above. These can be approximated by scaling the cross-sections in Fig. 20 by a ratio of the production rates that can be obtained from Fig. 15. We have computed the following Standard Model backgrounds to the signals:

(a) 1 - lepton events: W $\rightarrow$ e or μ + "jets" and $t\bar{t}$ production

(b) 2 - lepton events: $t\bar{t}$ production

For the background computation, we used a shower Monte-Carlo described in Ref. 31 for W and Z processes and the same experimental criteria as for the signal. We also computed the background from $t\bar{t}$ production for m_t = 60 and 120 GeV. The following comments are in order:

1. The backgrounds for 1 *lepton* + n *jets* + $E_T^{\rm miss}$ events appear to exceed signal for all choices of $M_{\tilde{g}}$, hence we have not illustrated this case. However, in the present analysis we have made no attempt at optimizing signal/background. Cutting on quantities such as M_T(e,$E_T^{\rm miss}$) or jet p_t may help in this matter. This is under study.
2. Signals for *two isolated leptons* + n *jets* + $E_T^{\rm miss}$

Table 5

Background rates from standard model processes for the signals shown in Figure 20. All numbers are in picobarns.

Isolated Dileptons + n JETS + $E_T^{\rm miss}$ ($E_T^{\rm miss}$ > 20 GeV)

# JETS	t(60)	t(120)
1	7	.3
2	4	.5
3	.7	.2
4	-	.002

events[33] exceed background only for $n \geq 4$. The cross-sections for two isolated leptons + 4 jets are typically in the range of ~0.01 pb so that at most a handful of these events may be expected. The cross-section for isolated same sign dileptons can exceed 0.1 pb and is as large as 0.01 pb even for $M_{\tilde{g}} = 200$ GeV. We were unable to find any background from $t\bar{t}$ for this class of events. A separate study, described in the next subsection, involved a more detailed analysis with different cuts, and also found optimistic results. Although the rate for these events is too small to envision that supersymmetry would be discovered in the dilepton channel, a handful of these clean events would provide a striking confirmation of a signal discovered in another channel.

To summarize, option B (a Tevatron upgrade to a pp collider operating at $\sqrt{s} = 2$ TeV and $\int$ Ldt = 1000 pb^{-1}) would give the highest event rate for gluinos if $M_{\tilde{g}} < 300$ GeV. Backgrounds should be more manageable because of lower W and Z production rates relative to a $p\bar{p}$ collider. Incorporating complete gluino cascade sequences in our programs yields new signatures for gluinos. The most promising are (1) isolated same sign dileptons + $E_T^{\rm miss}$ and (2) isolated dileptons + four or more jets + $E_T^{\rm miss}$. Each of these signals (along with the $E_T^{\rm miss}$ signal) should be present in a data sample if discovery of gluinos is to be claimed. More detailed studies of these signals are in progress.

4.6. Like-Sign Dileptons as a Signal for Gluino Production

In this section (following the work of Barnett, Gunion and Haber), we are interested in new gluino search techniques which could complement (or perhaps even substitute for) the standard missing-energy signature. One problem with the more complicated signatures is that, if seen, one must find means for identifying such a signal as being that of a gluino. Our approach will be to make use of a special feature of the gluino: it is a Majorana fermion. (Here, we use a broader definition of Majorana to include neutral particles which transform under real representations of the underlying Standard Model gauge group.) A very distinctive feature of a Majorana particle is that it can decay with equal probability into fermions and antifermions. Thus, we focus on a particular class of gluino decay chains such that $\tilde{g}\tilde{g}$ production will result in *like-sign* dileptons in the final state. Due to the Majorana nature of the gluino, the probability for the production of like-sign and opposite-sign leptons is equal, and the lepton decay characteristics of the two classes of final states are identical. This is quite a distinctive result, and if seen would be extremely helpful in identifying the origin of the events.

Consider as an example the decay $\tilde{g} \rightarrow q\bar{q}'\tilde{\chi}_1^{\pm}$, where $\tilde{\chi}_1^{\pm}$ is the lightest chargino state. As shown in Ref. 27, this decay mode is the dominant gluino decay (with branching ratio near 60%) over a large range of supersymmetric parameter space. The key point here is that the Majorana nature of the gluino implies that it is equally likely to decay into a chargino of either sign. The chargino decays dominantly into the LSP plus a real (or virtual) $W^{\pm}$, which then decays to electrons or muons 22% of the time. Thus the branching ratio for the decay chain $\tilde{g} \rightarrow q\bar{q}\ell^{\pm}\nu\tilde{\chi}_1^0$ is typically around 13%, with equal probability to produce a lepton of either sign. For simplicity, the τ–lepton will be neglected from our considerations. Since gluinos are produced in pairs (we assume that squarks are heavier so that $\tilde{q}\tilde{g}$ production can be ignored), this implies that the number of dilepton final states resulting from the decay of the two gluinos may be as large as 2% of all $\tilde{g}\tilde{g}$ events, of which half have like-sign leptons. Given the large cross-sections for gluino pair production at future colliders, there would exist a potentially large and interesting sample of events. This sample consists of events with hadronic jets (two from each gluino), missing energy due to the LSP and neutrinos in the final state, and a dilepton pair which can come in one of the following like-sign combinations: $e^{\pm}e^{\pm}$, $e^{\pm}\mu^{\pm}$, $\mu^{\pm}\mu^{\pm}$, and the corresponding opposite-sign combinations. Because the background is clearly larger for detecting the opposite-sign pairs, we shall focus here on the isolation of like-sign dilepton events originating from gluino pair production.

We have used a parton Monte Carlo in order to determine the viability of gluino detection using the like-sign dilepton signal. We have investigated the signal at the present Tevatron and at two future hadron colliders under consideration: an upgraded Tevatron and the SSC. Three Tevatron options are being considered, but we find that only the choice of a pp collider with $\sqrt{s} = 2\ TeV$ and an integrated luminosity of $1000pb^{-1}$ gives a significant improvement in discovery limits over the existing Tevatron. In addition to studying the characteristics of

the signal, we have tried to identify the major source of Standard Model background. In the case of the like-sign dilepton signal, the dominant background is expected to be $t\bar{t}$ production, where one t decays to $b\ell\nu$ and the other t decays to $b\bar{q}q'$ with the secondary b decaying into $c\ell\nu$. Such events will also produced like-sign dileptons (both muons and electrons), hadronic jets, and missing energy in the form of neutrinos. The background estimate will depend crucially on the unknown t-quark mass. We have studied two extreme cases in this regard: the "light" top ($m_t = 60\ GeV$) and the "heavy" top ($m_t = 160\ GeV$). We have identified a number of characteristics of the background that allow us to distinguish between it and the signal.

First, there is the lack of isolation of the lepton emitted from the b-quark. (We make use of the theoretical expectation that there is negligible mixing in neutral T-mesons which could cause primary like-sign dileptons in $t\bar{t}$ production from the t-quark decays.) This is to be compared with the case of dileptons from gluinos where both leptons resulting from the decay of a chargino (presumed to be much heavier than the b-quark) would be quite isolated. Thus we define $\Delta R_{l,j}^{min}$ to be the minimum $\Delta R \equiv \sqrt{(\Delta\eta)^2 + (\Delta\phi)^2}$ obtained by considering all lepton-jet combinations. Two other variables that allow us to discriminate against the background due to a top quark that is significantly lighter than the gluino are the total reconstructed mass of the event,

$$M_{tot}^2 = \left(\sum_{i=j_1,j_2,j_3,j_4,l_1,l_2} E_i + E_T^{\rm miss} \right)^2 - \left(\sum_{i=j_1,j_2,j_3,j_4,l_1,l_2} \vec{p}_i + \vec{p}_T^{\,miss} \right)^2 \qquad (4.13)$$

designed to approximate the total mass of the produced $\widetilde{g}\widetilde{g}$ system, and the invariant mass ($M_{l_2,2j}$) of the slow lepton and its two nearest (in ΔR) jets, which provides a measure of the invariant mass of the gluino. In Eq. (4.13) jets and leptons are labelled in order of decreasing transverse energy: $E_T^{j_1} > E_T^{j_2} > E_T^{j_3} > E_T^{j_4}$ and $E_T^{l_1} > E_T^{l_2}$.

Before presenting any details of the analysis we preview our conclusions. At the upgraded Tevatron option with an integrated luminosity of 1000 pb^{-1}, the like-sign dilepton signature is found to be viable for gluino masses up to 180 GeV. Of course, it is necessary to have a magnetic detector in order to be able to perform the type of analysis we describe here. Since it is clearly of interest to make sure that the SSC can probe down to this mass (so that there is no gap in accessible gluino masses for the combination of the two machines) we present the bulk of our results (both for an upgraded Tevatron and the SSC), assuming $M_{\widetilde{g}} = 180\ GeV$.

For simplicity, we employ the minimal supersymmetric extension of the Standard Model. Having specified $M_{\widetilde{g}}$, the remaining free parameters are μ, $\tan\beta$ and the mass of one of the Higgs bosons of the model (see Ref. 27 for notation). A particular choice of parameters can affect the chargino and neutralino mass spectrum and the gluino leptonic branching ratio. We have surveyed the supersymmetric parameter space and find that the gluino leptonic branching ratio is fairly stable over a considerable range of the parameters. We present results here for a typical choice: $\tan\beta = 1.5$, $m_{H^+} = 500\ GeV$, and $\mu = -150\ GeV$. For these values, we find $BR(\widetilde{g} \to \bar{q}q'\widetilde{\chi}_1^+) = 0.52$ and $BR(\widetilde{\chi}_1^+ \to \ell^\pm + \text{anything}) = 0.22$, where ℓ is either an electron or muon. Since in this case this is the only decay chain giving a single lepton, we find that like-sign dilepton events are 0.6% of all $\widetilde{g}\widetilde{g}$ events.

Let us first focus on the Tevatron upgrade analysis. First, we define a jet such that all parton jets within a cone of $\Delta R \leq 0.6$ around the jet axis are counted as one jet. We then employ the following cuts: (i) $N_{jet} \geq 4$, (ii) $E_T^{j_{1,2,3,4}} > 10\ GeV$, (iii) $N_{lepton} = 2$, and (iv) $E_T^{l_{1,2}} > 5\ GeV$. In addition, we impose a CDF-like trigger by requiring that at least one of the following three conditions be satisfied: (i) $E_T^{l_1} > 20\ GeV$, (ii) $E_T^{j_1} > 60\ GeV$, or (iii) $E_T^{j_{1,2,3}} > 20\ GeV$. Distributions in $\Delta R_{l,j}^{min}$, M_{tot}, $M_{l_2,2j}$ and $E_T^{l_2}$ are presented in Fig. 21. For the latter three we have plotted the $\widetilde{g}\widetilde{g}$ signal results before any $\Delta R_{l,j}^{min}$ cut (a $\Delta R_{l,j}^{min} > 0.48$ cut results in only a small decrease in the signal curve), in comparison to background results for $m_t = 60\ GeV$ with the $\Delta R_{l,j}^{min} > 0.48$ cut imposed and $m_t = 160\ GeV$ without any $\Delta R_{l,j}^{min}$ cut. All Tevatron curves are normalized to an integrated luminosity of 1000 pb^{-1}. The number of events in the $m_t = 60\ GeV$, $\Delta R_{l,j}^{min} > 0.48$ curves is 20, the number in the $m_t = 160\ GeV$, no $\Delta R_{l,j}^{min}$ cut curves is 91, while there are 18 and 14 events in the signal curve before and after the $\Delta R_{l,j}^{min}$ cut, respectively. For $m_t = 60\ GeV$ the background event rate is very high to begin with, but the $\Delta R_{l,j}^{min}$ cut is extremely effective in reducing it to the level of the signal. The mass distributions then allow one to easily distinguish between signal and background. At $m_t = 160\ GeV$ the background is not that much larger than signal and the $\Delta R_{l,j}^{min}$ distributions are sufficiently different to allow separation. Having made such a cut, the $E_T^{l_2}$ distributions of signal and background are quite different, as seen in Fig. 21b. On the other hand the mass distributions (Fig. 21c-d) are quite similar when $m_t \sim M_{\widetilde{g}}$. Note that in both cases, the gluino mass can be determined (within an accuracy of order 10%) from the M_{tot} distribution. These results from our upgraded Tevatron simulation show that the dilepton signature is marginal and requires large luminosity. The other proposed upgrades which do not plan for such a high integrated luminosity would not allow use of the dilepton

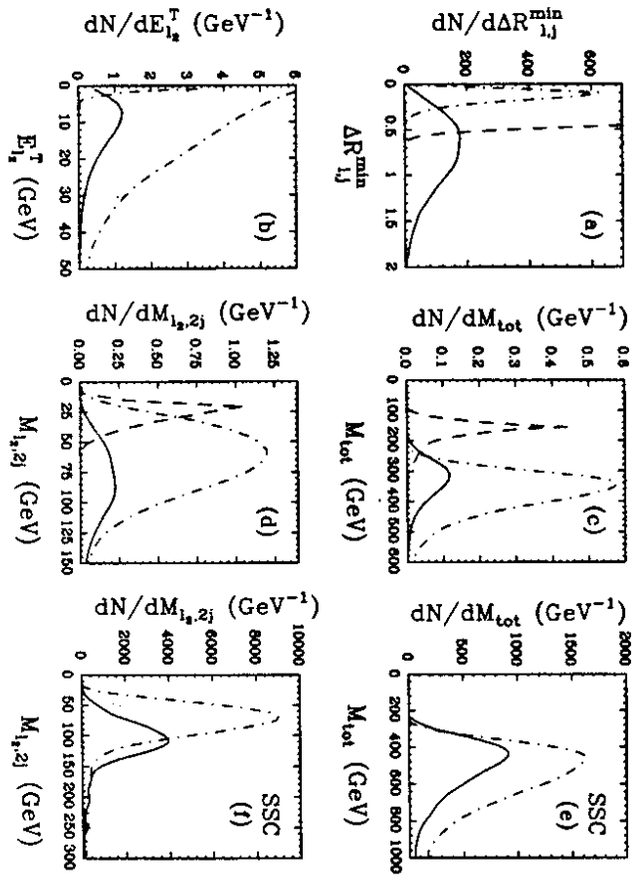

Figure 21. We present normalized distributions for the Tevatron upgrade, (a)-(d), and the SSC, (e) and (f), for $M_{\tilde{g}} = 180\ GeV$. All include the cuts and triggering conditions described in the text. The $\tilde{g}\tilde{g}$ signal curves are solid lines and have no $\Delta R_{l,j}^{min}$ cut; in (b)-(f) a $\Delta R_{l,j}^{min} > 0.48$ cut results in only a small decrease in the solid curve. Background curves for $m_t = 60\ GeV$ are dashed, while those for $m_t = 160\ GeV$ are dotdashed. The distributions are: (a) $\Delta R_{l,j}^{min}$ for the $\tilde{g}\tilde{g}$ signal multiplied by a factor of 10 compared to $m_t = 60\ GeV$ and $m_t = 160\ GeV$; (b) $E_T^{l_2}$ for $m_t = 160\ GeV$ before and after a $\Delta R_{l,j}^{min} > 0.48$ cut, compared to the $\tilde{g}\tilde{g}$ signal; (c) M_{tot} for $m_t = 60\ GeV$, $\Delta R_{l,j}^{min} > 0.48$, and $m_t = 160\ GeV$, no $\Delta R_{l,j}^{min}$ cut, compared to signal; (d) as in (c) but for $M_{l_2,2j}$; (e) M_{tot} for $m_t = 160\ GeV$, no $\Delta R_{l,j}^{min}$ cut, compared to signal; and (f) as in (e) but for $M_{l_2,2j}$.

signal to explore gluino masses as large as 180 GeV — the dilepton signal is essentially event rate limited.

We have also run our Monte Carlo under SSC conditions. We assume an integrated luminosity of $10^4\ pb^{-1}$. Since the raw $\tilde{g}\tilde{g}$ production rate is enormous for $M_{\tilde{g}} = 180\ GeV$ (yielding some 2.48×10^6 like-sign dilepton events before cuts), it is trivial to impose strong cuts on the $\Delta R_{l,j}^{min}$ and mass variables that completely eliminate any $m_t = 60\ GeV$ background. Thus, we focus on $m_t = 160\ GeV$. We employed a new set of cuts: (i) $N_{jet} \geq 4$, (ii) $E_T^{j_{1,2,3}} > 40\ GeV$, $E_T^{j_4} > 10\ GeV$, (iii) $N_{lepton} = 2$, and (iv) $E_T^{l_{1,2}} > 10\ GeV$. (Making a stronger cut on $E_T^{l_2}$ would completely eliminate the background. We have not done so in order to have some background to compare with our signal.) No trigger conditions were imposed. After the above cuts, we are left with 6×10^5 background events and 2.6×10^5 signal events. The $\Delta R_{l,j}^{min}$ distribution of the background is even more sharply peaked towards small $\Delta R_{l,j}^{min}$ in the SSC simulation than at the Tevatron, and would clearly allow isolation of the signal. The M_{tot} and $M_{l_2,2j}$ distributions for signal and background are shown in Fig. 21, with no $\Delta R_{l,j}^{min}$ cut imposed. We see that $M_{l_2,2j}$ also allows some discrimination. This SSC study suggests that we should even be able to isolate a gluino signal for gluinos lighter than 180 GeV.

We have also explored the maximum gluino mass that could be probed using the like-sign dilepton signature at the SSC.[34] For heavy gluinos the effective branching ratio for $\tilde{g}\tilde{g}$ final states containing like-sign electrons or muons and at least four energetic jets is typically of order 1% for a large range of parameter space. The large difference in $\Delta R_{l,j}^{min}$ distributions between signal and top backgrounds remains, and now the M_{tot} and $M_{l_2,2j}$ distributions for the $\tilde{g}\tilde{g}$ signal peak at such high masses that there is essentially no overlap with any $m_t < 200\ GeV$ background. Thus isolation of the signal is purely event rate limited. For $M_{\tilde{g}} = 2\ TeV$ and integrated luminosity of $10^4\ pb^{-1}$ there are 25 events in the dilepton signal, which would almost certainly allow discovery. Higher masses could be probed for larger integrated luminosities.

In conclusion, at an upgraded Tevatron with at least 1000 pb^{-1}, the like-sign dilepton signal may be visible for gluino masses up to 180 GeV, depending on the values of the other supersymmetric parameters. (Such a signal may even be observable at a Tevatron operating under present conditions for gluino masses near 90 GeV for special parameter choices.) At the SSC, the dilepton signal should be easy to detect for the entire range of gluino masses from $180 - 2000\ GeV$, very probably extending even lower. Such a copious like-sign dilepton signal would be strong evidence for phenomena related to a Majorana fermion, and the large event rates predicted here would almost surely allow experimenters to claim the discovery of the gluino, if such like-sign dilepton events were discovered. Clearly, the dilepton signal at the SSC is a powerful tool for uncovering evidence for supersymmetry.

5. Summary and Conclusions

Our study of the new particle discovery capabilities of the SSC indicates that it has a powerful potential to unravel many current mysteries of high energy physics. The range of masses to which it has access is enormous. Many types of signatures can be clearly separated from backgrounds. When new physics is discovered, it should be possible to establish not only its existence but also much about its nature. While we have not examined every possible type of new particle, the range of signals we studied was large, and probably includes signals expected from other particles.

The identification of new physics may require isolation of several signatures. This makes the achievement of design luminosity essential, because the branching ratios to given modes are often small. Among the many reasons why a *magnetic* detector is critical for finding new particles is the need to know the charge of leptons in multilepton events. We have shown that charge identification can be important both for eliminating backgrounds and for identifying the nature of the new physics. It should be emphasized that for many kinds of new physics the leptons are not fast (often $E_T^\ell \approx 20 - 100$ GeV) since they come from cascade decays. However, they are quite isolated compared with leptons from b decay. Leptons from new W' and Z' bosons might have p_T in the multi-TeV range, and sign determination for these may be unimportant. Because of the importance of decays with leptons and the small branching ratios to any given mode, it is essential to detect both electrons and muons in reasonable rapidity ranges. We have not directly addressed this issue in this particular study, but lepton coverage in $|\eta| < 3$ should be adequate. Note that in the supersymmetry section we found that the backgrounds for events with single leptons were too high so that the useful signals would be multi-lepton events; for these events the need for adequate rapidity coverage of electrons and muons is compounded. An issue which requires more attention is that of lepton misidentification; in particular, the mistaken labelling of isolated hadrons as leptons is a potential problem. We cannot say, for example, whether misidentification at the level of 10^{-3} is acceptable. The lepton and jet resolutions commonly discussed for SSC detectors appear to be sufficient for discovering most new particles. A role for vertex detection has not been suggested, but it may be useful in eliminating backgrounds. Further study is needed as to whether there will be problems triggering on some of the signatures proposed here and elsewhere.

We have shown here for the first time that new heavy leptons can be discovered at the SSC. New heavy bosons ($W'^{\pm}$ and Z'^0) are among the easiest particles to find at the SSC, and a high statistics study of asymmetries may yield useful information about their nature. For the first time we have performed detailed studies of the production of gluinos (the supersymmetric partner of the gluon) in which the small branching ratios were incorporated and in which full cascade decays were followed. We have emphasized the critical role of decays including leptons. The preliminary studies are very encouraging, leading us to believe that much can be learned about supersymmetry. High statistics ISAJET studies are proceeding.

We turn now to the issues concerning the proposed upgrades for the Tevatron Collider. There are motivations for upgrading the Tevatron Collider or for choosing one option over another option (accelerator technology, detector capabilities, etc.) beyond the purely physics issues raised here, but we have not addressed those questions at all. While the range of new particle masses available to an upgraded Tevatron Collider appears to be fully covered by existing facilities (including the existing Tevatron) plus the SSC, there may be valuable physics which could be done before the advent of the SSC. The excluded mass range for new particles such as new W' and Z' bosons, squarks and gluinos could be extended by 100-200 GeV. This can be compared with the SSC which will eventually extend these limits by 2000-7000 GeV. Of course it is also possible that these new particles have masses within the discovery reach of an upgraded Tevatron Collider. Some particles cannot be found at the Tevatron Collider because the luminosities proposed are inadequate for the combination of small production rates and very small branching ratios to any given mode. In fact the search range for most new physics is limited by luminosity.

The three upgrades options we considered were:

- Option A - A 2 TeV $p\bar{p}$ collider of luminosity 100 pb^{-1}.
- Option B - A 2 TeV pp collider of luminosity 1000 pb^{-1}.
- Option C - A 3 TeV $p\bar{p}$ collider of luminosity 30 pb^{-1}.

Which upgrade performs the best in new particle search and discovery depends largely on the mass of the particle. Furthermore, this question is dependent on whether just detection is sufficient or whether larger event rates are desired so that the properties of new particle can be studied. We found no circumstances in which Option A was preferable. The higher energy of Option C can lead to the highest search limits if and *only if* the resultant rate is adequate.

New heavy bosons (W' and Z') provide the one of the best possible examples of a favorable circumstance for Option C. Their production requires quark-antiquark annihilation thereby favoring a $p\bar{p}$ machine since it has a larger supply of antiquarks. However, the branching ratio to leptons is small, so even here Option C does not necessarily provide the best limits (based on 5 events), because of its limited luminosity. Option B is clearly preferred if 50 or more events are desired (in this latter case

the accessible masses are somewhat lower). Which option does best depends on the model and on model-dependent parameters. Option C tends to have the best discovery limits for new gauge bosons, although the differences are only 50 GeV or less. Looking at the forward-backward asymmetry, we see that for some choices of model parameters, it is considerably larger for $p\bar{p}$ machines, but this must be matched against the smaller event rates of Option C compared with Option B (at masses low enough to achieve event rates great enough to measure an asymmetry). If we compare the discovery limits of the upgrades to the limits from the current Tevatron Collider run (which we assume to have an integrated luminosity of 10 pb^{-1}), we find that the limits would be raised from about 550 GeV for W' bosons to about 800 GeV while the limits for Z' bosons would go from 400 to 600 GeV. For fixed boson masses of say 400 GeV, the upgrades yield about ten times as many events as the current run. Thus the potential for investigating new physics in the 1990s with Tevatron upgrades could be significant.

The production of other types of particles such as squarks and gluinos (the supersymmetric partners of the quarks and gluon) does not require quark-antiquark annihilation and in fact is dominated by production via gluons. In this case Option A does not surpass Option B for $\tilde{g}\tilde{g}$ production until the gluino mass is 380 GeV, and at that mass there is a fraction of an event per year for any given signal after branching ratios. For masses well below the discovery threshold, Option B has a tremendous advantage over the other options. For example, for $M_{\tilde{g}} = 150$ GeV Option B gives 26,000 gluino pairs per year (before any branching ratios) compared with 3200 and 5100 for Options A and C, respectively and with only 190 for the current Tevatron run with 10 pb^{-1}. At $M_{\tilde{g}} = 220$ GeV (which may be the discovery limit) the ratio of gluino pair production for Option B compared to Option C is 974 events to 381 events. The crossover point at which Option C begins to dominate Option B is about $M_{\tilde{g}} = 290$ GeV where about 50 total events per year would be produced; after branching ratios this rate is not adequate for discovery. Another measure of the difference for gluino production among the three options is a comparison of discovery reach. If Option B can achieve $M_{\tilde{g}} = 220$ GeV, then Option A can achieve 180 GeV, Option C 200 GeV and the current 10 pb^{-1} run 150 GeV. Incidentally for $M_{\tilde{g}} = 220$ GeV, the SSC would produce 2×10^8 events per year.

In conclusion, the potential for finding new physics at an upgraded Tevatron Collider is clearly far less than at the SSC, but several important discoveries might be within reach. In general we felt that Option B (with the highest luminosity) was a superior upgrade in the search for new particles. The differences in ultimate search limits were never great, but when larger event rates were required, Option B enjoyed a clear advantage. Option A seemed the least desirable. Finally, our group found that the SSC is essential in the search for the new particles which can solve some of the great puzzles of physics.

6. Acknowledgements

We would like to express our appreciation to the administrative, secretarial and computing staff of the Snowmass workshop for making the workshop a productive and enjoyable occasion. We also appreciate the effort of Sharon Jensen in helping the New Particles at Hadron Colliders group prepare this report and several other contributions. This work was supported by the Director, Office of Energy Research, Office of High Energy and Nuclear Physics, Division of High Energy Physics, of the U.S. Department of Energy under Contract Nos. DE-AC03-76SF00098, DE-AC02-76-ER0-3071, DE-AS03-76ER70191, DE-AA03-76-SF00010, DE-AC02-76ER00881 and W-7405-Eng-82, by the National Science Foundation under agreement no. PHY83-18358, and by the University of Wisconsin Research Committee with funds granted by the Wisconsin Alumni Research Foundation.

REFERENCES

1. E. Eichten *et al.*, *Rev. Mod. Phys.* **56**, 579 (1984).
2. D. Froidervaux in Proc. of the 1987 La Thuile Workshop on Physics at Future Accelerators, CERN 87/07.
3. V. Barger, Y. Han and J. Ohnemus, *Phys. Rev.* **D37**, 1134 (1988).
4. M.S. Chanowitz, M. Furman and I. Hinchliffe, *Nucl. Phys.* **B153**, 402 (1979), U. Amaldi, *et al.*, *Phys. Rev.* **D36**, 1385 (1987).
5. C. Albajar, *et al.*, *Phys. Lett.* **185B**, 241 (1987), *Phys. Lett.* **191B**, 463 (1987) (Erratum *Phys. Lett.* **197B**, 565 (1987)).
6. C. Hearty, *et al.*, *Phys. Rev. Lett.* **58**, 1711 (1987), C. Albajar, *et al.*, *Phys. Lett.* **198B**, 271 (1987).
7. Physics at LEP, ed. J. Ellis and R. Peccei, CERN 86-02.
8. S. Willenbrock and D. Dicus, *Phys. Lett.* **156B**, 429 (1987).
9. S. Dawson and S. Willenbrock, *Nucl. Phys.* **B284**, 449 (1987).
10. G. Alverson *et al.*, in Proc. of the 1986 DPF Summer Study on the Physics of the Superconducting Supercollider, Ed. J. Marx and R. Donaldson, FNAL (1987), J.F. Gunion and M. Soldate, *Phys. Rev.* **D34**, 826 (1986).
11. J.F. Gunion, G.L. Kane, H.F.W. Sadrozinski, A. Seiden, A.J. Weinstein, and C.P. Yuan, UCD-88-38, Nov 1988.

12. G. Alverson *et al.*, Ref. 10, H.-U. Bengtsson and A. Savoy-Navarro, *Phys. Rev.* **D37**, 1787 (1988)
13. M. Perl, *et al.*, *Phys. Lett.* **63B**, 466 (1976).
14. G. Marchesini and B. Webber, Cavendish preprint HEP 87/9 (1987), F. Paige and S.D. Protopopescu in Proc of 1986 in Proc. of the 1986 DPF Summer Study on the Physics of the Superconducting Supercollider, Ed. J. Marx and R. Donaldson, FNAL (1987), H.-U. Bengtsson and T. Sjostrand *Comp. Phys. Comm.* **46**,43 (1987).
15. J.C. Pati and A. Salam, *Phys. Rev.* **D10**, 275 (1974); R.N. Mohapatra and J.C.Pati, *Phys. Rev.* **D11** 566, 2558 (1975); G. Senjanovic and R.N. Mohapatra, *Phys. Rev.* **D12**, 1502 (1975). For a recent review, see R.N. Mohapatra in *Quarks, Leptons and Beyond*, ed. H. Fritzsch *et al.*, Plenum, New York (1985), p. 217.
16. N.G. Deshpande, J.A. Grifols and A. Méndez, *Phys.Lett.* **208B**, 141 (1988).
17. J.F. Gunion, J.A. Grifols, A.Mendez, B. Kayser and F. Olness; UCD preprint in preparation.
18. J. L. Hewett and T. G. Rizzo, Univ. Wisconsin report MAD/PH/446, submitted to Physics Reports (1988).
19. For a general survey of the left-right Symmetric Model, its basis in SO(10) and original references see R. N. Mohapatra, *Unification and Supersymmetry*, Springer- Verlag, New York, 1986.
20. E. Ma, Phys. Rev. **D36**, 274 1987 ; Mod. Phys. Lett. **A3**, 319 (1988); K. S. Babu, X.-G. He, and E. Ma, Phys. Rev. **D36**, 878 (1987); J. F. Gunion *et al.*, *Proceedings of the Workshop From Colliders to Supercolliders*, Madison, WI, May (1987) and Int. J. Mod. Phys. **A2**, 119 (1987); V. Barger and K. Whisnant, *ibid.* **A3**, 879 (1988).
21. The problems associated with a measurement of A_{FB}^{ℓ} for new Z' bosons has been discussed earlier by H. Haber, New W and Z Group Summary, *Proceedings of the 1984 Summer Study on the Design and Utilization of the SSC*, Snowmass, CO, 1984, edited by R. Donaldson and J. Morfin.
22. C. Albajar et al., Phys. Lett. **B198**, 261 (1987)
23. J. Freeman and F. Abe et al., Proceedings of the 7th International Conference on $\bar{p}p$ Collisions, Fermilab, June, 1988 (preliminary).
24. See H.E. Haber and G.L. Kane, Phys. Rep. **117**, 75 (1985) and references therein.
25. R. Batley, in *Proc. of the 1987 La Thuile Workshop on Physics at Future Accelerators*, Vol. 2, ed. J.H. Mulvey, CERN 87-07 (1987), p.109; R.M. Barnett, H.E. Haber and G.L. Kane, Phys. Rev. Lett. **54**, 1983 (1985) and Nucl. Phys. **B267**, 625 (1986); H. Baer, J. Ellis, G. Gelmini, D. Nanopoulos and X. Tata, Phys. Lett. **161B**, 175 (1985); G. Gamberini, Z Phys. **C30**, 605 (1986); H. Baer, V. Barger, D. Karatas and X. Tata, Phys. Rev. **D36**, 96 (1987).
26. G. Gamberini, Z. Phys. **C30**, 605 (1986); H. Baer and E.L. Berger, Phys. Rev. **D34**, 1361 (1986); H. Baer, V. Barger, D. Karatas and X. Tata, Phys. Rev. **D36**, 96 (1987); R. Barbieri, G. Gamberini, G.F. Giudice and G. Ridolfi, Nucl. Phys. **B301**, 15 (1988).
27. R.M. Barnett, J.F. Gunion and H.E. Haber, Phys. Rev. Lett. **60**, 401 (1988); Phys. Rev. **D37**, 1892 (1988).
28. H. Baer, J. Ellis, G. Gelmini, D. Nanopoulos and X. Tata, Phys. Lett. **161B**, 175 (1985); R.M. Barnett, H.E. Haber and G.L. Kane, Phys. Rev. Lett. **54**, 1983 (1985) and Nucl. Phys. **B267**, 625 (1986); G. Gamberini, Z Phys. **C30**, 605 (1986); H. Baer, V. Barger, D. Karatas and X. Tata, Phys. Rev. **D36**, 96 (1987); R.M. Barnett, J.F. Gunion and H.E. Haber, Phys. Rev. **D37**, 1892 (1988).
29. J. Gunion, et.al., in *From Colliders to Supercolliders*, pg. 255 edited by V. Barger and F. Halzen, published by World Scientific; J. Gunion and H. Haber, Phys. Rev. **D37**, 2515 (1988).
30. H. Baer, K. Hagiwara and X. Tata, Phys. Rev. **D38**, 1485 (1988).
31. H. Baer, V. Barger, H. Goldberg and R. Phillips, Phys. Rev. **D37**, 3152 (1988).
32. V. Barger, T. Gottschalk, J. Ohnemus and R. Phillips, Phys. Rev. **D32**, 2950 (1985).
33. V. Barger, W.Y. Keung and R. Phillips, Phys. Rev. Lett. **55**, 166 (1985); see R.M. Barnett, J.F. Gunion and H.E. Haber, these proceedings.
34. For a somewhat more extensive survey of the high mass region at future hadron colliders, see J.F. Gunion, "INFN Eloisatron Project Working Group Report", Erice-Trapani (1988).

LAWRENCE BERKELEY LABORATORY
TECHNICAL INFORMATION DEPARTMENT
1 CYCLOTRON ROAD
BERKELEY, CALIFORNIA 94720